

The Euclidean quantisation of Kerr-Newman-de Sitter black holes*

Piotr T. Chruściel[†] and Michael Hörzinger
Erwin Schrödinger Institute and Faculty of Physics
University of Vienna

March 6, 2022

Abstract

We study the family of Einstein-Maxwell instantons associated with the Kerr-Newman metrics with a positive cosmological constant. This leads to a quantisation condition on the masses, charges, and angular momentum parameters of the resulting Euclidean solutions.

Contents

Contents	1
1 Introduction	2
2 The fields	3
3 Regularity at the rotation axes	5
3.1 $a = 0$	7
3.2 $a \neq 0$: the quantisation conditions	7
3.3 Maxwell fields	8
4 Topology	9
5 The solutions	10
6 The limit $n_1 \rightarrow \infty$	12
7 Dirac strings	17
A A typical solution	19
B Physical quantities	20
B.1 Euclidean case	20
B.2 Lorentzian case	21
C A sample	22

*Preprint UWThPh-2015-32

[†]Email piotr.chrusciel@univie.ac.at, URL <http://homepage.univie.ac.at/piotr.chrusciel>

D SI units	22
E Lorentzian partner solutions	24
E.1 Geometric units	25
E.2 SI units, $\Lambda = 1.11 \times 10^{-52} m^{-2}$	25
F Page limit	26
E1 Parametrization of r_0 and a by v and \bar{e}	28
F.1.1 Magnetic charge equal to electric charge (possibly zero) .	29
F.1.2 $\bar{e} > 0$	29
F.1.3 $\bar{e} < 0$	30
E2 The Maxwell fields in the Page limit	30
E3 Dirac strings	33
References	33

1 Introduction

Euclidean counterparts of Lorentzian solutions play an important role in Euclidean Quantum Gravity [8, 10]. It appears therefore of interest to find Euclidean versions of key Lorentzian solutions.

As such, Kerr-Newman solutions have a unique position in view of their uniqueness properties. The associated solutions with positive cosmological constant, discovered by Demiański and Plebański [18] and, independently, by Carter [2], are similarly expected to be unique under natural conditions. Surprisingly enough, their compact Euclidean counterparts do not seem to have been explored in the literature. The object of this paper is to fill this gap.

More precisely, we construct two new families of compact Riemannian four-dimensional manifolds satisfying the Einstein-Maxwell equations with a positive cosmological constant. The solutions are obtained by complex substitutions in the Kerr-Newman de Sitter metric. The requirement of smoothness and compactness of the underlying manifold leads to a quantisation condition on the mass and charge parameters of the associated Lorentzian manifold. We thus obtain our first family of metrics, on S^2 - and \mathbb{RP}^2 -bundles over S^2 , parameterised by two integers (n_1, n_2) . The second family is parameterised by a single integer $n \in \mathbb{N}$ and is obtained by passing to a limit *à la Page* in the Euclidean Kerr-Newman de Sitter metrics. We determine several physical parameters associated with the Lorentzian equivalents of the solutions and study their asymptotics as one, or both, parameters tend to infinity. We calculate the associated Euclidean actions, which determine the contribution of our instantons to the Euclidean path integral in a saddle point approximation, as well as horizon entropies and temperatures.

Our Riemannian solutions $({}^4M, g)$ have a clear quantum relevance. On a more mundane level, since the Maxwell energy-momentum tensor has vanishing trace, the metrics we have constructed provide time-symmetric initial data for the $4 + 1$ vacuum Einstein equations with a positive cosmological constant, or for Einstein equations with matter (e.g., dust) having constant density on the initial data surface 4M . Indeed, the four-dimensional Euclidean Einstein-Maxwell equations imply that the four-dimensional Riemannian metric g has constant positive scalar curvature. Therefore the initial data set $({}^4M, g, K = 0)$ satisfies the $4 + 1$ vacuum time-symmetric constraint equations with a positive cosmological constant, or $4 + 1$ time-symmetric constraint

equations with dust which has constant density, or with a constant scalar field, or with a mixture of the above.

The solutions in our first family are uniquely parameterized by the already mentioned quantum numbers $(n_1, n_2) \in \mathbb{N}^2$, $1 \leq n_2 < n_1$, and the value of the cosmological constant Λ . It might be viewed as amusing, and perhaps not entirely unexpected, that after inserting the experimentally determined value of Λ , the masses of all Lorentzian solutions associated with our Euclidean ones are of the same order as some standard current estimates, based on the FLRW model, for the total mass of the visible universe.

The quantum numbers (n_1, n_2) , resulting from the requirement of regularity of the Riemannian manifold, lead to a quantisation of the mass, the angular momentum, and the combination $p^2 - e^2$ of the magnetic charge parameter p and electric charge parameter e . We show that the requirement of a well-defined test Dirac field with charge q_0 on the Riemannian manifold introduces two further quantum numbers (\hat{n}_1, \hat{n}_2) , together with a quantisation of e , p and q_0 .

2 The fields

The Kerr-Newman-de Sitter (KNdS) metric is a solution of the Einstein-Maxwell equations,

$$R_{\mu\nu} - \frac{1}{2}g_{\mu\nu}R + \Lambda g_{\mu\nu} = 8\pi T_{\mu\nu}, \quad dF = 0, \quad d \star F = 0, \quad (2.1)$$

where Λ is the cosmological constant (which we assume to be positive throughout this work), and where

$$T_{\mu\nu} = \frac{1}{4\pi}(F_{\mu\rho}F_{\nu}{}^{\rho} - \frac{1}{4}F^{\alpha\beta}F_{\alpha\beta}g_{\mu\nu}). \quad (2.2)$$

In Boyer-Lindquist coordinates, after the replacement $a \rightarrow ia$, $t \rightarrow it$ and $e \rightarrow ie$ the metric takes the form¹

$$g = \frac{\Sigma}{\Delta_r}dr^2 + \frac{\Sigma}{\Delta_\theta}d\theta^2 + \frac{\sin^2(\theta)}{\Xi^2\Sigma}\Delta_\theta(adt + (r^2 - a^2)d\varphi)^2 + \frac{1}{\Xi^2\Sigma}\Delta_r(dt - a\sin^2(\theta)d\varphi)^2, \quad (2.3)$$

where, setting $\lambda = \Lambda/3$,

$$\Sigma = r^2 - a^2 \cos^2(\theta), \quad \Delta_r = (r^2 - a^2)(1 - \lambda r^2) - 2Mr + p^2 - e^2, \quad (2.4)$$

$$\Delta_\theta = 1 - \lambda a^2 \cos^2(\theta), \quad \Xi = 1 - \lambda a^2. \quad (2.5)$$

The Maxwell potential reads

$$A = \frac{p \cos(\theta)}{\Sigma}\sigma_1 + \frac{er}{\Sigma}\sigma_2, \quad (2.6)$$

¹In geometric considerations below it is convenient to scale the objects involved so that all coordinates, as well as a , M , e , p and Λ are unitless. When translating back to SI units in the Lorentzian metric, it is useful to observe that Δ_r/r^2 has no dimensions. Thus, if r is instead measured in meters then λr^2 , which is one of the summands of Δ_r/r^2 , must have no dimension and thus λ must have dimension m^{-2} , etc.

where the one-forms σ_i , $i = 1, 2$, are defined as

$$\sigma_1 = \frac{1}{\Xi} (-a dt - (r^2 - a^2) d\varphi), \quad \sigma_2 = \frac{1}{\Xi} (-dt + a \sin^2(\theta) d\varphi). \quad (2.7)$$

Now, each metric (2.3) is determined uniquely by the parameters a , M , and the combination

$$p_{\text{eff}}^2 := p^2 - e^2. \quad (2.8)$$

of the magnetic charge parameter p and the electric charge parameter e . The notation in (2.8) might appear to be misleading, because the right-hand side of this equation could be negative. However, it turns out to be mostly appropriate, in that we have not found any non-singular solutions with $p^2 \leq e^2$ using our procedure below except in the Page limit discussed in Appendix F.

We emphasise that *any* pairs (e, p) satisfying (2.8) are allowed. When transforming back to the Lorentzian regime, there is no ambiguity in determining the parameters M and a characterising the Lorentzian solution, which remain unchanged. On the other hand, if we denote by p_L and e_L the parameters characterising the Maxwell field on the Lorentzian side, then *any* values of p_L and e_L satisfying

$$p_L^2 + e_L^2 = p^2 + e^2 \quad (2.9)$$

are compatible with the Einstein-Maxwell equations for the *Lorentzian metric*. The question thus arises whether, given a set (a, M, e, p) arising from a Riemannian metric, there is a preferred choice of p_L and e_L .

A natural choice is

$$p_L = p, \quad e_L = e. \quad (2.10)$$

The condition $p_{\text{eff}}^2 > 0$ and (2.8) imply that the simplest choice $p_L = 0$ in (2.10) is not possible, except in the Page limit. The next simplest choice, $e_L = 0$, leads then to purely magnetic solutions with a quantised magnetic charge. We emphasise that our quantisation mechanism of magnetic charge has nothing to do with the Dirac one, see Section 7 below.

Whether or not (2.10) is the right choice appears to be a matter of debate, see [6, 11]. An alternative would be to decree that the Lorentzian solutions with $p_L = 0$ and $e_L \neq 0$ correspond to Riemannian solutions for which $\hat{A} := e_L r \sigma_2 / \Sigma$ is a vector potential for

$$\star F_{\mu\nu} := \frac{1}{2} \epsilon_{\mu\nu}^{\alpha\beta} F_{\alpha\beta} = \partial_\mu \hat{A}_\nu - \partial_\nu \hat{A}_\mu, \quad (2.11)$$

where $\epsilon_{\mu\nu\alpha\beta}$ is the totally antisymmetric tensor. In this case $p_{\text{eff}}^2 = e_L^2$ (compare [6]). This choice leads to a quantisation of electric charge.

It might be of interest to note that *planar Lorentz transformations* of (p, e) preserve p_{eff}^2 and can be thought of as the Euclidean counterparts of the usual duality transformations of the Maxwell field, which instead act as rotations of the (p, e) plane.

In any case, we wish to find ranges of parameters so that (2.3) is a Riemannian metric on a closed manifold M . This leads to the following obvious restrictions:

First, compactness requires φ and t to be periodic, with a period which needs to be determined.

Further, compactness of M requires a range of the variable r , bounded by two *first-order zeros* $r_1 < r_2$ of Δ_r , so that (2.3) is Riemannian for $\forall r \in$

(r_1, r_2) , $\theta \in (0, \pi)$.² In particular

$$\frac{\Sigma}{\Delta_r} > 0 \quad \text{and} \quad \frac{\Sigma}{\Delta_\theta} > 0 \quad \forall r \in (r_1, r_2), \theta \in (0, \pi). \quad (2.12)$$

Equations (2.4) and (2.5) show that Σ and Δ_θ are positive on the equatorial plane, and we conclude that

$$\Delta_r > 0, \quad \Sigma > 0 \quad \text{and} \quad \Delta_\theta > 0 \quad \forall r \in (r_1, r_2), \theta \in (0, \pi). \quad (2.13)$$

Now, if $r_1 r_2 \leq 0$, then $0 \in [r_1, r_2]$, and since $\Sigma|_{r=0} < 0$ this case will not lead to a regular Riemannian metric. Changing r to its negative, it remains to consider the case where $0 < r_1 < r_2$. Positivity of Σ leads then to $r_1 > |a|$, and positivity of Δ_θ imposes the restriction $\lambda^{-1} > a^2$. Summarising:

$$0 < |a| < r_1 < r_2, \quad a^2 < \lambda^{-1}, \quad \Delta_r|_{(r_1, r_2)} > 0. \quad (2.14)$$

Given a Euclidean metric as above *with* $e = 0$, the corresponding Lorentzian metric with the same real values of λ , M , a , $e = 0$, and p will be called a *partner solution*. Note that the locations r_i of the horizons of the partner solution will *not* coincide with the locations r_i of the rotation axes of the associated Euclidean solutions; similarly for areas, surface gravities, etc.

3 Regularity at the rotation axes

For $r \in [r_1, r_2]$ let us introduce two functions ρ_i , $i = 1, 2$, defined as

$$\rho_i = \epsilon_i \int_{r_i}^r \frac{1}{\sqrt{\Delta_r}} dr = \frac{2}{\sqrt{\lambda_i}} \sqrt{\epsilon_i(r - r_i)} \mathbb{1}_{1,i}(r - r_i), \quad (3.1)$$

with $\epsilon_1 = 1$, $\epsilon_2 = -1$, and

$$\lambda_i := |\Delta'_r|_{r=r_i} \neq 0, \quad i = 1, 2, \quad (3.2)$$

and with functions $\mathbb{1}_{1,i}$ which are smooth near the origin and satisfy $\mathbb{1}_{1,i}(0) = 1$. The function ρ_1 will serve as a coordinate replacing r for $r \in [r_1, r_2)$, while ρ_2 will replace r for $r \in (r_1, r_2]$. Inverting, it follows that

$$r = r_1 + \frac{\lambda_1}{4} \rho_1^2 \mathbb{1}_2(\rho_1^2), \quad \Delta_r = \frac{\lambda_1^2}{4} \rho_1^2 \mathbb{1}_3(\rho_1^2), \quad (3.3)$$

with functions $\mathbb{1}_2, \mathbb{1}_3$ which are smooth near the origin, with $\mathbb{1}_2(0) = 1 = \mathbb{1}_3(0)$.

In order to make sure that the metric is regular near the intersection of the axes $\{\sin \theta = 0\}$ with the axes $\{\Delta_r = 0\}$, near $\theta = 0$ and for $r \in [r_1, r_2)$ we use a coordinate system $(\rho_1, t_1, \theta, \phi_1)$, with $t = \omega_1 t_1$ and φ defined through the formula

$$d\varphi := \alpha_1 d\phi_1 + \frac{a}{a^2 - r_1^2} dt \equiv \alpha_1 d\phi_1 + \frac{a\omega_1}{a^2 - r_1^2} dt_1, \quad (3.4)$$

for some constants $\alpha_1, \omega_1 \in \mathbb{R}^*$ which will be determined shortly by requiring 2π -periodicity of t_1 and ϕ_1 . In (3.4) the coefficient in front of dt has been

²One can likewise enquire about existence of compact Euclidean solutions with $\Lambda \leq 0$. One easily checks that for $\Lambda \leq 0$ the function Δ_r has no maxima in the range of parameters of interest, and therefore no configurations as considered here exist.

chosen so that $g_{tt}|_{\rho_1=0} = 0$. In this coordinate system the metric takes the form

$$g = \Sigma \left\{ d\rho_1^2 + \frac{1}{\Xi^2 \Sigma^2} \left[\frac{\lambda_1^2 \omega_1^2 \Sigma^2}{4(r_1^2 - a^2)^2} \mathbb{I}_4(\rho_1^2, \sin^2(\theta)) \rho_1^2 dt_1^2 \right. \right. \\ \left. \left. + \alpha_1^2 (\Delta_\theta (a^2 - r^2)^2 + a^2 \Delta_r \sin^2(\theta)) \sin^2(\theta) d\phi_1^2 \right. \right. \\ \left. \left. + F(\rho_1^2, \sin^2(\theta)) \rho_1^2 \sin^2(\theta) dt_1 d\phi_1 \right] + \frac{1}{\Delta_\theta} d\theta^2 \right\}, \quad (3.5)$$

for some smooth functions \mathbb{I}_4 and F , with $\mathbb{I}_4(0, y) = 1$. As is well known, when (ρ_1, t_1) are viewed as polar coordinates around $\rho_1 = 0$, the one form $\rho_1^2 dt_1$ and the quadratic form $d\rho_1^2 + \rho_1^2 dt_1^2$ are smooth. Similarly when (θ, ϕ_1) are polar coordinates around $\theta = 0$, the one form $\sin^2(\theta) d\phi_1$ and the quadratic form $d\theta^2 + \sin^2(\theta) d\phi_1^2$ are smooth. It is then easily inferred that the requirements of 2π -periodicity of t_1 and ϕ_1 , together with

$$\frac{\lambda_1^2 \omega_1^2}{4\Xi^2 (r_1^2 - a^2)^2} = 1, \quad \frac{\alpha_1^2 \Delta_\theta^2 (a^2 - r^2)^2}{\Xi^2 (r^2 - a^2 \cos^2(\theta))^2} \Big|_{\theta=0} = 1, \quad (3.6)$$

implies smoothness both of the sum of the diagonal terms of the metric g and of the off-diagonal term $g_{t_1 \phi_1} dt_1 d\phi_1$ on

$$\{(r, t_1, \theta, \phi_1) \in [r_1, r_2] \times S^1 \times [0, \pi] \times S^1\}.$$

Note that (3.6) is equivalent to

$$\omega_1 = \pm \underbrace{\frac{2\Xi(r_1^2 - a^2)}{\lambda_1}}_{=: \omega}, \quad \alpha_1 = \pm 1. \quad (3.7)$$

The above calculations remain valid without changes near $\theta = \pi$. It is, however, convenient, to use a different symbol for the resulting polar coordinates: When $\theta \in (0, \pi]$ we will use \hat{t}_1 and $\hat{\phi}_1$ for the relevant angular coordinates, and $\hat{\omega}_1, \hat{\alpha}_1$ for the corresponding coefficients. Thus, for $\theta \in (0, \pi]$:

$$t = \hat{\omega}_1 \hat{t}_1, \quad d\varphi = \hat{\alpha}_1 d\hat{\phi}_1 + \frac{a\hat{\omega}_1}{a^2 - r_1^2} d\hat{t}_1, \quad (3.8)$$

with

$$\hat{\omega}_1 = \pm \omega, \quad \hat{\alpha}_1 = \pm 1. \quad (3.9)$$

Identical considerations for $r \in (r_1, r_2]$, using coordinate systems $(\rho_2, t_2 = t\omega_2^{-1}, \theta, \phi_2)$ for $\theta \in [0, \pi)$ and $(\rho_2, \hat{t}_2 = t\hat{\omega}_2^{-1}, \theta, \hat{\phi}_2)$ for $\theta \in (0, \pi]$, with

$$d\varphi = \alpha_2 d\phi_2 + \frac{a\omega_2}{a^2 - r_2^2} dt_2, \quad d\varphi = \hat{\alpha}_2 d\hat{\phi}_2 + \frac{a\hat{\omega}_2}{a^2 - r_2^2} d\hat{t}_2, \quad (3.10)$$

lead to

$$\omega_2, \hat{\omega}_2 \in \left\{ \pm \frac{2\Xi(r_2^2 - a^2)}{\lambda_2} \right\}, \quad \alpha_2, \hat{\alpha}_2 \in \{\pm 1\}. \quad (3.11)$$

In an overlap region where both t and t_1 are coordinates, the equation $t = \omega_1 t_1$ implies that t must be exactly $2\pi|\omega_1|$ -periodic. Similarly, in any overlap region where both t and t_2 are defined and are coordinates, t must be exactly $2\pi|\omega_2|$ -periodic. A similar argument applies to \hat{t}_i . So, the periodicity requirements of t_i and \hat{t}_i lead to

$$\omega_1 = \pm \omega_2, \quad \hat{\omega}_1 = \pm \hat{\omega}_2. \quad (3.12)$$

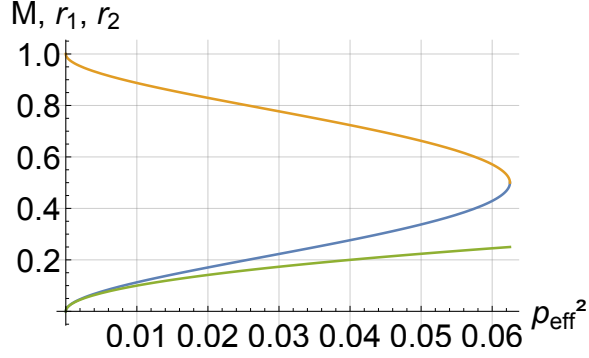


Figure 3.1: Solutions with $a = 0$ scaled to $\lambda = 1$. The uppermost curve is a plot of r_2 , the middle one that of r_1 , the lowest curve is a plot of the mass parameter M .

3.1 $a = 0$

When $a = 0$, and imposing the regularity conditions above, the metric (3.13) simplifies considerably:

$$g = r^2 \left\{ d\rho_1^2 + \mathbb{I}_4(\rho_1^2, \sin^2(\theta)) \rho_1^2 dt_1^2 + d\theta^2 + \sin^2(\theta) d\phi_1^2 \right\}. \quad (3.13)$$

The coordinate ρ_1 can be written explicitly in terms of elliptic integrals, which is not very enlightening.

After scaling to $\lambda = 1$, the periodicity conditions (3.12) are verified by a one-parameter family of solutions parameterized by a continuous parameter $p_{\text{eff}}^2 \in [0, 1/16]$, see Figure 3.1. These solutions will not be discussed any further.

3.2 $a \neq 0$: the quantisation conditions

When $a \neq 0$, without loss of generality, replacing t and/or φ by their negatives if necessary, we require

$$a > 0, \quad \omega_1 = \omega > 0. \quad (3.14)$$

To avoid ambiguities: except for the analysis of the Page limit in Appendix F, in what follows we will assume that (r, t, θ, φ) form a *smooth coordinate system away from the rotation axes*, with t and φ periodic.

Increasing ϕ_1 from zero to 2π with (ρ_1, t_1, θ) fixed takes one back to the starting point. Equations (3.4) and (3.7) show that φ changes by $\pm 2\pi$, and therefore the minimal period of φ must be $2\pi/k$ for some $k \in \mathbb{N}^*$. But then, increasing φ from zero to $2\pi/k$ with (r, t, θ) fixed takes one to the same place. This results in an increase of ϕ_1 by $\pm 2\pi/k$, which implies that $k = 1$. Hence, φ is exactly 2π -periodic.

Now, increasing t_1 from zero to 2π with φ_1 fixed again takes one to the same place. This implies that φ must have changed by an integer multiple of 2π .

The same argument applies to φ_2 and t_2 . We conclude that

$$n_i := \frac{a\omega}{r_i^2 - a^2} \in \mathbb{N}^*. \quad (3.15)$$

3.3 Maxwell fields

Let us check that the Maxwell fields, defined as dA away from all axes of rotation, extend by continuity to smooth fields once the above constraints have been imposed. This can be done by inspection of the Maxwell potentials (2.6) (which, incidentally, are *not* regular at the rotation axes).

We start with an analysis of the p -contribution to A which, using (3.4) and its equivalent with r_1 replaced by r_2 , can be rewritten as

$$\begin{aligned}
\frac{p \cos(\theta)}{\Sigma} \sigma_1 &= \frac{p \cos(\theta)}{\Xi \Sigma} (-a dt - (r^2 - a^2) d\varphi) \\
&= \frac{p \cos(\theta)}{\Xi \Sigma} \left(-a dt - (r^2 - a^2) \left(\alpha_i d\phi_i + \frac{a}{a^2 - r_i^2} dt \right) \right) \\
&= \frac{p \cos(\theta)}{\Xi \Sigma} \left(\frac{a(r^2 - r_i^2)}{r_i^2 - a^2} dt - \alpha_i (r^2 - a^2) d\phi_i \right) \\
&= \underbrace{\frac{p \cos(\theta)}{\Xi} \left(\frac{a(r^2 - r_i^2)}{\Sigma(r_i^2 - a^2)} dt + \frac{\alpha_i a^2 \sin^2 \theta}{r^2 - a^2 \cos^2(\theta)} d\phi_i \right)}_{\text{smooth}} - \frac{\alpha_i p \cos(\theta)}{\Xi} d\phi_i \quad (3.16)
\end{aligned}$$

where the index i on r_i , α_i and ϕ_i takes the values $i \in \{1, 2\}$. More precisely, the underbraced term in the last line of (3.16) is smooth away from $r = r_2$ when $i = 1$, and away from $r = r_1$ when $i = 2$. Near the axis $\cos \theta = 1$ the last, *non-smooth* term can be rewritten as

$$-\frac{\alpha_i p \cos(\theta)}{\Xi} d\phi_i = -\underbrace{\frac{\alpha_i p (\cos(\theta) - 1)}{\Xi} d\phi_i}_{\text{smooth for } \theta < \pi} - \underbrace{\frac{\alpha_i p}{\Xi} d\phi_i}_{\text{closed}}, \quad (3.17)$$

which shows smoothness of the p -contribution to $F = dA$ near $\theta = 0$.

In fact, we have proved that, for $i = 1, 2$, the vector potentials

$$\frac{p \cos(\theta)}{\Sigma} \sigma_1 + \frac{\alpha_i p}{\Xi} d\phi_i = \frac{p \cos(\theta)}{\Sigma} \sigma_1 + \frac{p}{\Xi} \left(d\varphi - \frac{a}{a^2 - r_i^2} dt \right) \quad (3.18)$$

which are well-defined and smooth away from all axes of rotation, extend by continuity across $\theta = 0$ and $r = r_i$ to smooth covector fields.

An identical calculation near the axis $\cos \theta = -1$, with ϕ_i replaced by $\hat{\phi}_i$, shows that the offending term can be rewritten as

$$-\frac{\alpha_i p \cos(\theta)}{\Xi} d\hat{\phi}_i = -\underbrace{\frac{\alpha_i p (\cos(\theta) + 1)}{\Xi} d\hat{\phi}_i}_{\text{smooth for } \theta > 0} - \underbrace{\frac{\alpha_i p}{\Xi} d\hat{\phi}_i}_{\text{closed}}, \quad (3.19)$$

which finishes the proof of smoothness of the p -contribution to F everywhere. We also see that the potentials

$$\frac{p \cos(\theta)}{\Sigma} \sigma_1 - \frac{\alpha_i p}{\Xi} d\hat{\phi}_i = \frac{p \cos(\theta)}{\Sigma} \sigma_1 - \frac{p}{\Xi} \left(d\varphi - \frac{a}{a^2 - r_i^2} dt \right) \quad (3.20)$$

extend smoothly to the axis $\theta = \pi$.

We continue with the e -contribution to A :

$$\frac{e r}{\Sigma} \sigma_2 = \frac{e r}{\Sigma \Xi} (-dt + a \sin^2(\theta) d\varphi) = \frac{e r}{\Sigma \Xi} \left(-dt + a \sin^2(\theta) \left(\alpha_i d\phi_i + \frac{a}{a^2 - r_i^2} dt \right) \right)$$

$$\begin{aligned}
&= \frac{e r}{\Sigma \Xi} \left(\frac{r_i^2 - a^2 \cos^2(\theta)}{a^2 - r_i^2} dt + a \alpha_i \sin^2(\theta) d\phi_i \right) \\
&= \frac{e}{\Xi} \left(\frac{r_i^2 - a^2 \cos^2(\theta)}{r^2 - a^2 \cos^2(\theta)} \times \frac{r}{(a^2 - r_i^2)} dt + \frac{\alpha_i a r \sin^2(\theta)}{r^2 - a^2 \cos^2(\theta)} d\phi_i \right) \\
&= \frac{e}{\Xi} \left(\left(1 - \frac{r^2 - r_i^2}{r^2 - a^2 \cos^2(\theta)} \right) \frac{r}{(a^2 - r_i^2)} dt + \frac{\alpha_i a r \sin^2(\theta)}{r^2 - a^2 \cos^2(\theta)} d\phi_i \right) \\
&= \frac{e}{\Xi} \underbrace{\left(\frac{r - r_i}{(a^2 - r_i^2)} dt - \frac{r^2 - r_i^2}{r^2 - a^2 \cos^2(\theta)} \times \frac{r}{(a^2 - r_i^2)} dt + \frac{\alpha_i a r \sin^2(\theta)}{r^2 - a^2 \cos^2(\theta)} d\phi_i \right)}_{\text{smooth near } r = r_i} \\
&\quad + \underbrace{\frac{e r_i}{\Xi(a^2 - r_i^2)} dt}_{\text{closed}}. \tag{3.21}
\end{aligned}$$

This finishes the proof of smoothness of F .

Note that (3.21) shows that $e r \sigma_2 / \Sigma$ extends smoothly across both $\theta = 0$ and $\theta = \pi$ without further due as long as one stays away from the axes $r \in \{r_1, r_2\}$.

4 Topology

The results of Section 3 can be summarised as follows: imposing 2π -periodicity of $t_1, \hat{t}_1, t_2, \hat{t}_2, \varphi_1, \hat{\varphi}_1, \varphi_2$ and $\hat{\varphi}_2$, together with $\omega_1 = \omega$, and $\hat{\omega}_1, \omega_2, \hat{\omega}_2 \in \{\pm\omega\}$, as well as $\alpha_1, \hat{\alpha}_1, \alpha_2, \hat{\alpha}_2 \in \{\pm 1\}$ and (3.15), the coordinates $(\rho_i, t_i, \theta, \varphi_i)$, $(\rho_i, \hat{t}_i, \theta, \hat{\varphi}_i)$, $i = 1, 2$ such that

$$\rho_i(r) = \int_{r_i}^r \frac{1}{\sqrt{\Delta_r}} dr, \quad \omega t_1 = t = \pm \omega t_2, \tag{4.1}$$

$$\alpha_1 d\phi_1 + \frac{a\omega}{r_1^2 - a^2} dt_1 = d\varphi = \alpha_2 d\phi_2 \pm \frac{a\omega}{r_2^2 - a^2} dt_2, \tag{4.2}$$

similarly for the hatted ones, provide polar coordinates on the following four distinct coordinate patches, each containing exactly one intersection of the axes of rotation $\{\Delta_r = 0\} \cap \{\sin(\theta) = 0\}$ in their centers:

$$\Omega_{r_1,0} := [r_1, r_2]_{\rho_1} \times S_{t_1}^1 \times [0, \pi]_{\theta} \times S_{\phi_1}^1 \approx D_{(\rho_1, t_1)}^2 \times D_{(\theta, \phi_1)}^2, \tag{4.3}$$

$$\Omega_{r_2,0} := (r_1, r_2]_{\rho_2} \times S_{t_2}^1 \times [0, \pi]_{\theta} \times S_{\phi_2}^1 \approx D_{(\rho_2, t_2)}^2 \times D_{(\theta, \phi_2)}^2, \tag{4.4}$$

$$\Omega_{r_1,\pi} := [r_1, r_2]_{\rho_1} \times S_{\hat{t}_1}^1 \times (0, \pi]_{\theta} \times S_{\hat{\phi}_1}^1 \approx D_{(\rho_1, \hat{t}_1)}^2 \times D_{(\theta, \hat{\phi}_1)}^2, \tag{4.5}$$

$$\Omega_{r_2,\pi} := (r_1, r_2]_{\rho_2} \times S_{\hat{t}_2}^1 \times (0, \pi]_{\theta} \times S_{\hat{\phi}_2}^1 \approx D_{(\rho_2, \hat{t}_2)}^2 \times D_{(\theta, \hat{\phi}_2)}^2. \tag{4.6}$$

Here “ \approx ” means “diffeomorphic to”, and $D_{(\rho_1, t_1)}^2$ denotes an open disc $D^2 \subset \mathbb{R}^2$ coordinatised by polar coordinates (ρ_1, t_1) while $S_{t_2}^1$ denotes a circle S^1 coordinatised by t_2 , etc. Quite generally, we use the notation U_x to denote the fact that a set U is coordinatised by a variable x .

The question then arises, in how many ways can one glue the sets above to obtain smooth closed manifolds. We point out some possible constructions here. While we suspect that these are all possibilities, we have not made in-depth attempts to analyse whether or not the list below is exhaustive.³ Note that oriented manifolds are obtained if and only if $\omega_2 = \alpha_1 \alpha_2 \omega$.

³The solutions we construct are $U(1) \times U(1)$ -symmetric, and the results in [15] are relevant in this context. However, one could also search for manifolds carrying the metric (2.3) which are only locally $U(1) \times U(1)$ -symmetric.

1. We can glue $\Omega_{r_1,0}$ with $\Omega_{r_1,\pi}$ by identifying for $\theta \in (0, \pi)$ the points $(\rho_1, t_1, \theta, \phi_1)$ with $(\rho_1, \hat{t}_1, \theta, \phi_1)$; similarly for $\Omega_{r_2,0}$ and $\Omega_{r_2,\pi}$. This corresponds to the choice $\alpha_1 = \alpha_2$, and leads to the manifolds

$$\hat{\Omega}_1^+ := [r_1, r_2]_{\rho_1} \times S_{t_1}^1 \times [0, \pi]_{\theta} \times S_{\phi_1}^1 \approx D_{(\rho_1, t_1)}^2 \times S_{(\theta, \phi_1)}^2,$$

as well as

$$\hat{\Omega}_2^+ := (r_1, r_2]_{\rho_2} \times S_{t_2}^1 \times [0, \pi]_{\theta} \times S_{\phi_2}^1 \approx D_{(\rho_2, t_2)}^2 \times S_{(\theta, \phi_2)}^2,$$

where S^2 denotes a two-dimensional sphere.

Since the map $\theta \rightarrow \pi - \theta$ is an isometry, a second possibility in the same spirit is to identify for $\theta \in (0, \pi)$ the points $(\rho_1, t_1, \theta, \phi_1)$ with $(\rho_1, \hat{t}_1, \pi - \theta, \phi_1 + \pi)$. This leads to \mathbb{RP}^2 bundles over $D_{(\rho_1, t_1)}^2$ and $D_{(\rho_2, t_2)}^2$, which are not orientable.

2. Let us set

$$\zeta := \omega_2 / \omega_1 \in \{\pm 1\} \quad \Rightarrow \quad dt_1 = \zeta dt_2. \quad (4.7)$$

Consider the manifolds $\hat{\Omega}_i^+$, $i = 1, 2$. Both are trivial S^2 bundles over the open disc D^2 . Near the boundary of D^2 , for each t_2 the corresponding sphere at t_1 is obtained by rotating S^2 around the z -axis by an angle $\alpha_1 \zeta (n_2 - n_1) t_2$:

$$\alpha_1 d\phi_1 + n_1 dt_1 = \alpha_2 d\phi_2 + \zeta n_2 dt_2 \quad \Rightarrow \quad \phi_1 = \alpha_1 \alpha_2 \phi_2 + \alpha_1 \zeta (n_2 - n_1) t_2 + c, \quad (4.8)$$

for some constant c . So, as we circle around the boundary of D^2 , the sphere S^2 is rotated by a total angle $2\alpha_1 \zeta (n_2 - n_1) \pi$ during each revolution. The end manifold is a non-trivial sphere bundle over S^2 when $n_2 - n_1$ is odd.

A similar construction applies to the \mathbb{RP}^2 bundles above.

3. Let $(\rho_1)_{\max}$ be the maximal value of the coordinate ρ_1 , thus

$$\begin{aligned} \rho_1(r) &= \int_{r_i}^r \frac{1}{\sqrt{\Delta_r}} dr = \underbrace{\int_{r_{1i}}^{r_2} \frac{1}{\sqrt{\Delta_r}} dr}_{=(\rho_1)_{\max}} - \underbrace{\int_r^{r_2} \frac{1}{\sqrt{\Delta_r}} dr}_{=\rho_2} \\ &= (\rho_1)_{\max} - \rho_2, \end{aligned} \quad (4.9)$$

and suppose that the map

$$(\rho_1 = \rho, t_1 = s) \mapsto (\rho_1 = (\rho_1)_{\max} - \rho, t_1 = s + \pi)$$

is an isometry. This, however, occurs for the metrics considered here only in the Page limit, and is therefore only relevant to Appendix F. Then the identification of $(\rho_1, t_1, \theta, \phi_1)$ with

$$(\rho_2 = (\rho_1)_{\max} - \rho_1, \hat{t}_2 = t_1 + \pi, \pi - \theta, n(\phi_1 + \pi))$$

leads to a smooth compact manifold.

5 The solutions

The question then arises to find values of (M, p_{eff}^2, a) so that

$$\omega_1 = \zeta \omega_2, \quad \zeta \in \{\pm 1\}, \quad \frac{a\omega_1}{r_1^2 - a^2} = n_1 \in \mathbb{N}^*, \quad \frac{a|\omega_2|}{r_2^2 - a^2} = n_2 \in \mathbb{N}^*. \quad (5.1)$$

It follows from (3.7) and (3.11) that the above equations are equivalent to

$$\frac{(r_1^2 - a^2) \Delta'_r(r_2)}{(r_2^2 - a^2) \Delta'_r(r_1)} = -1, \quad \Delta'_r(r_1) n_1 = 2a\Xi, \quad -\Delta'_r(r_2) n_2 = 2a\Xi. \quad (5.2)$$

In addition we need to fulfill $\Delta_r(r_i) = 0$, leading to the system of polynomial equations for $(r_1, r_2, n_1, n_2, a, M, p_{\text{eff}}^2)$.

$$\Delta_r(r_1) = 0, \quad (5.3)$$

$$\Delta_r(r_2) = 0, \quad (5.4)$$

$$\Delta'_r(r_1) n_1 - 2a\Xi = 0, \quad (5.5)$$

$$-\Delta'_r(r_2) n_2 - 2a\Xi = 0, \quad (5.6)$$

$$(r_1^2 - a^2) n_1 - (r_2^2 - a^2) n_2 = 0. \quad (5.7)$$

Note that $n_1 > n_2 \geq 1$ in view of (5.7). Moreover the solutions have to satisfy the constraints

- i) $M \in \mathbb{R}, a > 0, p_{\text{eff}}^2 \in \mathbb{R};$
- ii) $n_1, n_2 \in \mathbb{N}^*;$
- iii) $0 < r_1 < r_2, |a| < |r_1|$ and $a^2 < \lambda^{-1}$.

We note that we also need $\forall r \in (r_1, r_2) : \Delta_r(r) > 0$, but this follows from the fact that $\Delta'_r(r_1)$ is positive by (5.5) and $\Delta'_r(r_2)$ is negative by (5.6).

We also note that equations (5.3)-(5.7) involve neither ζ nor the α_i 's as in (4.7)-(4.8), which can thus be arbitrarily chosen once a solution has been found.

Our strategy is to prescribe $\lambda \in \mathbb{R}_+^*$, $n_1, n_2 \in \mathbb{N}^*$ so that (5.3)-(5.7) become a system of five polynomials in the variables $(r_1, r_2, p_{\text{eff}}^2, M, a)$. We use MATHEMATICA to compute a Gröbner basis of the system. This provides a simpler equivalent system to solve. It turns out that one is led to a hierarchic system of polynomial equations, the first one depending only on p_{eff}^2 , the second one only on p_{eff}^2 and a , and so forth. An example is provided in Appendix A.

Our MATHEMATICA calculations show the following: Let

$$n_{\text{max}} = 50. \quad (5.8)$$

Then:

1. There exist no solutions with $(n_1, n_2) \in \mathbb{N} \times \mathbb{N}$ with $1 \leq n_2 < n_1 \leq n_{\text{max}}$ and $p_{\text{eff}}^2 \leq 0$. In particular there are no vacuum solutions with the properties set forth above.
2. For every pair $(n_1, n_2) \in \mathbb{N} \times \mathbb{N}$ with $1 \leq n_2 < n_1 \leq n_{\text{max}}$ there exists exactly one solution satisfying our constraints.
3. The physical parameters (see Appendix B) of the Lorentzian partner solutions are all bounded, cf. Table 5.1. In particular the physical mass of the Lorentzian partners is strictly positive, bounded away from zero, and bounded from above.

It should be emphasised that the existence of the solutions of the system as above is a rigorous result, derived by exact computer algebra. While numerics is used to check whether the joint zeros of the Gröbner basis satisfy the desired inequalities, this is again a rigorous statement, as the numerical errors introduced when checking the inequalities are well below the gaps occurring in the inequalities.

	$(n_1, n_2)_{\min}$	min.		$(n_1, n_2)_{\max}$	max.
$ q_{\text{phys}} $	(2, 1)	0.2511	$ q_{\text{phys}} $	(∞, ∞)	$\frac{\sqrt{2}}{3} \approx 0.47$
M_{phys}	$(\infty, 1)$	0.2036	M_{phys}	(100, 90)	0.2548
$ J_{\text{phys}} $	(2, 1)	0.01392	$ J_{\text{phys}} $	(∞, ∞)	$\frac{1}{9} \approx 0.111$
S	(2, 1)	-2.357	S	(∞, n_2)	∞

Table 5.1: Left table: Minimal values of the effective physical Lorentzian charge $|q_{\text{phys}}|$, the physical mass M_{phys} , the physical angular momentum $|J_{\text{phys}}|$, and the Euclidean action S with the corresponding quantum numbers $(n_1, n_2)_{\min}$. Right table: Maximal values of $|q_{\text{phys}}| := \sqrt{p_{\text{eff}}^2/(1+a^2)}$, M_{phys} , $|J_{\text{phys}}|$, S with the corresponding quantum numbers $(n_1, n_2)_{\max}$. All values scaled to $\lambda = 1$; compare Appendix D.

We expect that the threshold (5.8) is irrelevant, and indeed we have randomly sampled many further values of (n_1, n_2) , including e.g.

$$(n_2, n_1) \in \{(1, 10000), (20, 1000), (200, 1000), (1000, 10000)\},$$

with the same result. Plots displaying various correlations between parameters are shown in Figure 5.1. The plots show that the resulting parameters (a, M, p_{eff}^2) are bounded, and that the values of the parameters approach affine correlations as both n_1 and n_2 tend to infinity. This is explained in Section 6 below, where exact bounds and the asymptotically affine relations are derived.

6 The limit $n_1 \rightarrow \infty$

An interesting case arises when we require $r = a$ to be a double zero of Δ_r . While in this case the geometry is not compact anymore, the resulting manifold provides a description of the geometry which is approached when n_1 tends to infinity with n_2 kept fixed. The values of the parameters (a, m, p_{eff}^2) which arise in this case correspond to the limiting curves which arise in the plots showing the correlations between the parameters.

In order to study the system (5.3-5.7) for large n_1 , we rewrite (5.7) in the form

$$(r_1^2 - a^2) - (r_2^2 - a^2) \frac{n_2}{n_1} = 0. \quad (6.1)$$

Passing to the limit $n_1 \rightarrow \infty$ with n_2 fixed one is led to

$$0 = r_1^2 - a^2 = \Delta'_r(r_1) = \Delta_r(r_1) = \Delta_r(r_2) = -\Delta'_r(r_2)n_2 - 2a\Xi. \quad (6.2)$$

In particular $r_1 = a$. Scaling the metric by a constant so that $\Lambda = 3$, and using $r_1 = a$ in Eq.(5.5) we obtain $M = a(1 - a^2)$. Injecting in (5.3) gives $p_{\text{eff}}^2 = 2a^2(a^2 - 1)$. Summarising

$$r_1 = a, \quad M = a(1 - a^2), \quad p_{\text{eff}}^2 = 2a^2(1 - a^2). \quad (6.3)$$

The parameter a can then be determined using

$$\Delta_r(r_2) = 0 = \Delta'_r(r_2)n_2 + 2a\Xi, \quad (6.4)$$

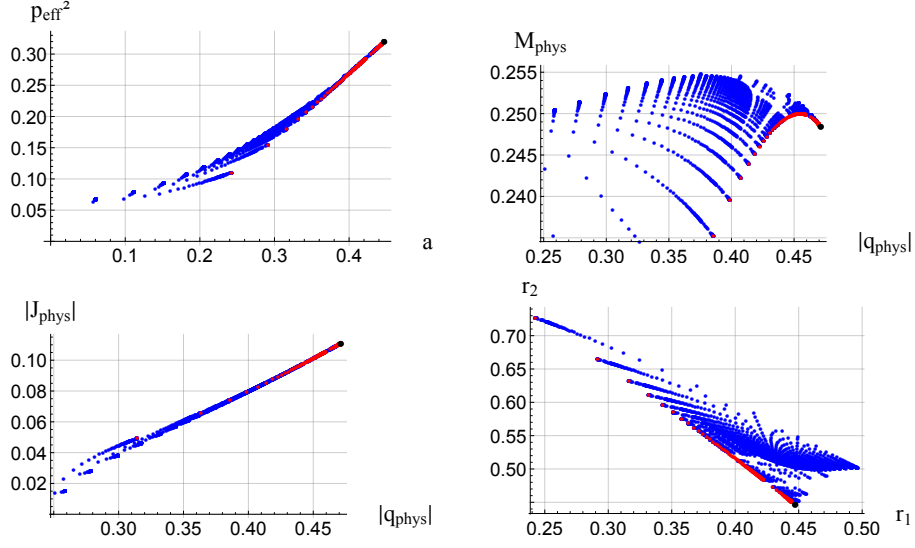


Figure 5.1: Correlations between a and p_{eff}^2 (upper left plot), $|q_{\text{phys}}|$ and M_{phys} (upper right), $|q_{\text{phys}}|$ and $|J_{\text{phys}}|$ (lower left), and r_1 vs. r_2 (lower right plot). The blue dots correspond to about 2000 solutions which are obtained by taking all values of $1 \leq n_2 < n_1 \leq 50$ and a sample of values in the range $1 \leq n_2 < n_1 \leq 1000$. The red dots are obtained by letting $n_1 \rightarrow \infty$ (cf. Section 6), with $1 \leq n_2 \leq 9900$. The black dot is the limit $n_1 \rightarrow \infty$, $n_2 \rightarrow \infty$ (cf. Section 6).

with M and p_{eff}^2 given by (6.3). Some algebra gives

$$a = \sqrt{\frac{2n_2(5n_2 - 2\sqrt{8n_2 + 1} + 4) - \sqrt{8n_2 + 1} + 1}{2n_2(25n_2 + 8) + 2}}, \quad (6.5)$$

$$r_2 = \frac{(2n_2 + \sqrt{8n_2 + 1} + 1) \sqrt{\frac{4n_2(5n_2 - 2\sqrt{8n_2 + 1} + 4) - 2\sqrt{8n_2 + 1} + 2}{n_2(25n_2 + 8) + 1}}}{4n_2}. \quad (6.6)$$

The corresponding physical parameters are

$$M_{\text{phys}} = \frac{a(1 - a^2)}{(1 + a^2)^2}, \quad |J_{\text{phys}}| = \frac{a^2(1 - a^2)}{(1 + a^2)^2}, \quad |q_{\text{phys}}| = \frac{a\sqrt{2(1 - a^2)}}{(1 + a^2)}. \quad (6.7)$$

Here $M_{\text{phys}} = M/(1 + \lambda a^2)^2$ is the *physical mass* of the Lorentzian partner solution (compare [3, 9]), $|J_{\text{phys}}| = aM/(1 + \lambda a^2)$ is the *Komar angular momentum* of the Lorentzian partner solution, and $|q_{\text{phys}}| := \sqrt{p_{\text{eff}}^2}/(1 + \lambda a^2)$ is the *total magnetic Maxwell charge* of the Lorentzian solution with $e = 0$ (compare [19]).

We have

$$\Delta_r''|_{r=a} = 2 - 10a^2,$$

so that Δ_r is positive for $0 < a < r_2$, with a simple zero at $r = r_2$, if and only if

$$0 < a < \frac{1}{\sqrt{5}}. \quad (6.8)$$

Inspection of (2.3) shows that the metric g is complete, with a smooth axis of rotation at the other zero $r = r_2$ of Δ_r when $n_2 \in \mathbb{Z}$. The set $r = a$ is infinitely

far away, with the region $r \rightarrow a$ displaying an interesting geometry: While the circles of constant t , r and $\theta \notin \{0, \pi\}$ shrink to zero as r tends to a , the metric on the spheres of constant φ and r is stretched along the meridians and approaches a smooth Riemannian metric on a cylinder obtained by removing the north and south pole from S^2 .

We have the following expansions, for large $n_2 \in \mathbb{N}$,

$$\begin{aligned}
a &= \sqrt{\frac{2n_2(5n_2 - 2\sqrt{8n_2 + 1} + 4) - \sqrt{8n_2 + 1} + 1}{2n_2(25n_2 + 8) + 2}} \\
&= \frac{1}{\sqrt{5}} - \frac{2}{5}\sqrt{\frac{2}{5}}\sqrt{\frac{1}{n_2}} + \frac{2}{25\sqrt{5}n_2} + \frac{7}{100\sqrt{10}}\left(\frac{1}{n_2}\right)^{3/2} + O(n_2^{-2}) \\
&\rightarrow_{n_2 \rightarrow \infty} \frac{1}{\sqrt{5}} \approx 0.45,
\end{aligned} \tag{6.9}$$

$$\begin{aligned}
M &= \sqrt{\frac{(2n_2(5n_2 - 2\sqrt{8n_2 + 1} + 4) - \sqrt{8n_2 + 1} + 1)}{8(n_2(25n_2 + 8) + 1)^3}} \times \\
&\quad \times (4n_2(10n_2 + \sqrt{8n_2 + 1} + 2) + \sqrt{8n_2 + 1} + 1) \\
&= \frac{4}{5\sqrt{5}} - \frac{4}{25}\sqrt{\frac{2}{5}}\sqrt{\frac{1}{n_2}} - \frac{4}{25\sqrt{5}n_2} + \frac{39}{250\sqrt{10}}\left(\frac{1}{n_2}\right)^{3/2} + O(n_2^{-2}) \\
&\rightarrow_{n_2 \rightarrow \infty} \frac{4}{5\sqrt{5}} \approx 0.36,
\end{aligned} \tag{6.10}$$

$$\begin{aligned}
p_{\text{eff}}^2 &= \frac{n_2^2(4n_2(50n_2 - 15\sqrt{8n_2 + 1} + 34) - 15\sqrt{8n_2 + 1} + 17)}{(n_2(25n_2 + 8) + 1)^2} \\
&= \frac{1}{\sqrt{5}} - \frac{2}{5}\sqrt{\frac{2}{5}}\sqrt{\frac{1}{n_2}} + \frac{2}{25\sqrt{5}n_2} + \frac{7}{100\sqrt{10}}\left(\frac{1}{n_2}\right)^{3/2} + O(n_2^{-2}) \\
&\rightarrow_{n_2 \rightarrow \infty} \frac{8}{25} \approx 0.32,
\end{aligned} \tag{6.11}$$

$$\begin{aligned}
M_{\text{phys}} &= \frac{4n_2(10n_2 + \sqrt{8n_2 + 1} + 2) + \sqrt{8n_2 + 1} + 1}{(4n_2(-15n_2 + \sqrt{8n_2 + 1} - 6) + \sqrt{8n_2 + 1} - 3)^2} \\
&\quad \times \sqrt{2(n_2(25n_2 + 8) + 1)(2n_2(5n_2 - 2\sqrt{8n_2 + 1} + 4) - \sqrt{8n_2 + 1} + 1)} \\
&= \frac{\sqrt{5}}{9} + \frac{1}{27}\sqrt{\frac{2}{5}}\sqrt{\frac{1}{n_2}} - \frac{1}{5\sqrt{5}n_2} + \frac{421}{48600\sqrt{10}}\left(\frac{1}{n_2}\right)^{3/2} + \frac{8867}{145800\sqrt{5}n_2^2} - O(n_2^{-5/2}) \\
&\rightarrow_{n_2 \rightarrow \infty} \frac{\sqrt{5}}{9} \approx 0.25,
\end{aligned} \tag{6.13}$$

$$\begin{aligned}
|J_{\text{phys}}| &= \frac{8n_2^2}{4n_2(18n_2 + 3\sqrt{8n_2 + 1} + 10) + 3\sqrt{8n_2 + 1} + 5} \\
&= \frac{1}{9} - \frac{1}{27}\sqrt{2}\sqrt{\frac{1}{n_2}} - \frac{1}{27n_2} + \frac{83}{1944\sqrt{2}}\left(\frac{1}{n_2}\right)^{3/2} + \frac{37}{5832n_2^2} + O(n_2^{-5/2}) \\
&\rightarrow_{n_2 \rightarrow \infty} \frac{1}{9},
\end{aligned} \tag{6.14}$$

$$\begin{aligned}
|q_{\text{phys}}| &= \frac{2(n_2(25n_2 + 8) + 1)}{4n_2(15n_2 - \sqrt{8n_2 + 1} + 6) - \sqrt{8n_2 + 1} + 3} \\
&\quad \times \sqrt{\frac{n_2^2(4n_2(50n_2 - 15\sqrt{8n_2 + 1} + 34) - 15\sqrt{8n_2 + 1} + 17)}{(n_2(25n_2 + 8) + 1)^2}}
\end{aligned} \tag{6.16}$$

$$\begin{aligned}
&= \frac{\sqrt{2}}{3} - \frac{1}{9} \sqrt{\frac{1}{n_2}} - \frac{7}{54\sqrt{2}n_2} + \frac{55}{1296} \left(\frac{1}{n_2}\right)^{3/2} + \frac{5}{243\sqrt{2}n_2^2} + O(n_2^{-5/2}) \\
&\rightarrow_{n_2 \rightarrow \infty} \frac{\sqrt{2}}{3} \approx 0.471.
\end{aligned} \tag{6.17}$$

Perhaps surprisingly, the total volume of the solutions (directly related to the gravitational contribution S_G to the action, see (B.5) below) turns out to be finite. To determine it we use (B.3) below with $\kappa = |\kappa_2|$, which equals

$$\begin{aligned}
\kappa_2 &= \frac{-2r_2(r_2^2 - a^2) + 2a(a^2 - 1) + 2r_2(1 - r_2^2)}{2(1 - a^2)(r_2^2 - a^2)} \\
&= -\frac{1}{2} \sqrt{\frac{5}{2}} \sqrt{\frac{1}{n_2}} + \frac{7}{8\sqrt{5}n_2} + O(n_2^{-3/2}).
\end{aligned} \tag{6.18}$$

One finds

$$\begin{aligned}
V &= \frac{\pi^2(4n_2 + \sqrt{8n_2 + 1} - 1)}{3n_2} \\
&= \frac{4\pi^2}{3} + \frac{4\pi^2}{3\sqrt{2}} \sqrt{\frac{1}{n_2}} - \frac{\pi^2}{3n_2} + O(n_2^{-3/2}) \\
&\rightarrow_{n_2 \rightarrow \infty} \frac{4\pi^2}{3} \approx 13.16.
\end{aligned} \tag{6.19}$$

Plots showing monotonicity of some of the functions above, at least for n_2 large enough, can be found in Figure 6.1. A plot of S_G as a function of n_2 can be found in Figure 6.2.

M_{phys} attains its maximum at $n_2 = \sqrt{\frac{1}{2}(799 + 565\sqrt{2})} + 10\sqrt{2} + 14 \approx 56.409$, at which point it equals $1/4$. Closer inspection, taking into account that we are only interested in integer values of n_2 , gives

$$0.20361015 \approx M_{\text{phys}}|_{n_2=1} \leq M_{\text{phys}} \leq M_{\text{phys}}|_{n_2=56} \approx 0.24999998, \tag{6.20}$$

with the bounds being optimal.

All quantities have an asymptotic expansion, as n_2 tends to infinity, in terms of negative powers of $\sqrt{n_2}$. This leads to simple relations between various quantities for n_1 and n_2 large, as follows: for large n_2 we have the approximate relations

$$\begin{aligned}
\sqrt{\frac{1}{n_2}} &\approx \frac{5}{2} \sqrt{\frac{5}{2}} \left(\frac{1}{\sqrt{5}} - a \right) \approx \frac{25}{4} \sqrt{\frac{5}{2}} \left(\frac{4}{5\sqrt{5}} - M \right) \approx \frac{5}{2} \sqrt{\frac{5}{2}} \left(\frac{1}{\sqrt{5}} - p_{\text{eff}}^2 \right) \approx \frac{2\sqrt{2}}{\pi} \left(-\frac{\pi}{2} - S_G \right) \\
&\approx 27 \sqrt{\frac{5}{2}} \left(M_{\text{phys}} - \frac{\sqrt{5}}{9} \right) \approx \frac{27}{\sqrt{2}} \left(\frac{1}{9} - |J_{\text{phys}}| \right) \approx 9 \left(-\frac{\sqrt{3}}{2} - |q_{\text{phys}}| \right).
\end{aligned} \tag{6.21}$$

From this one obtains various approximately affine relations between the quantities above for $1 \ll n_1 \ll n_2$, e.g.

$$|J_{\text{phys}}| \approx -\sqrt{5}M_{\text{phys}} + \frac{2}{3}, \tag{6.22}$$

$$|q_{\text{phys}}| \approx -\frac{9}{3}M_{\text{phys}} + \frac{\sqrt{2} - \sqrt{5}}{3}, \tag{6.23}$$

$$S_G \approx -\frac{\sqrt{5}\pi}{4}M_{\text{phys}} - \frac{13}{36}\pi. \tag{6.24}$$

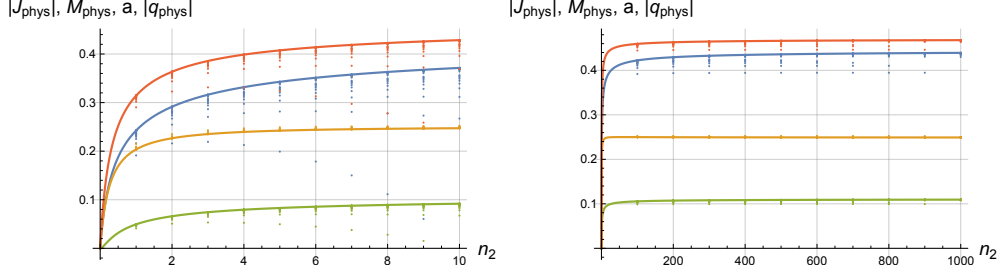


Figure 6.1: Plots of $|J_{\text{phys}}|$ (lowest curve), M_{phys} (next to lowest on the left plot), a (next to highest curve), and $|q_{\text{phys}}|$ (highest curve) as functions of a continuous variable $n_2 \in [0, 10]$ (left plot) and $n_2 \in [0, 1000]$ (right plot). The dots correspond to the values obtained for the solutions with the given values of n_2 and with n_1 increasing in logarithmic steps to 10000 (left plot) and 100000 (right plot).

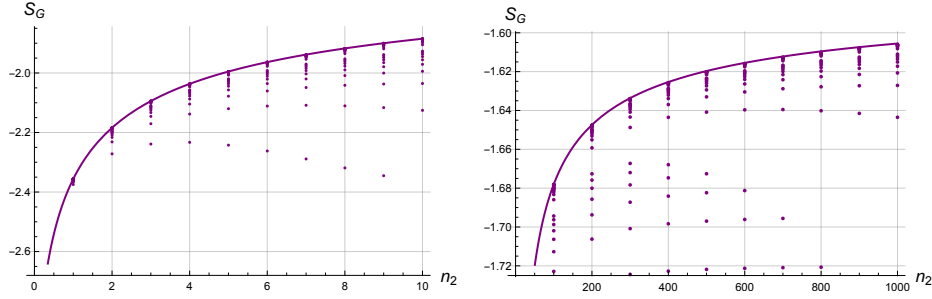


Figure 6.2: Plots of the gravitational contribution $S_G = -\Lambda V/(8\pi)$, scaled to $\Lambda = 3$, to the Euclidean action S as function of a continuous variable $n_2 \in [0, 10]$ (left plot) and $n_2 \in [0, 1000]$ (right plot). The dots correspond to the values obtained for the solutions with the given values of n_2 and with n_1 increasing in logarithmic steps to 10000 (left plot) and 100000 (right plot).

One can similarly make a second-order approximation in $1/n$, by expanding the quantities of interest up to $o(n^{-1})$ and eliminating n from the equations. As an example, near the maximum value of $|q_{\text{phys}}|$ we obtain the relation

$$M_{\text{phys}} \approx \frac{3402\sqrt{2}|q_{\text{phys}}| + 394\sqrt{3}\sqrt{5 - 7\sqrt{2}|q_{\text{phys}}|} - 1437}{2205\sqrt{5}}. \quad (6.25)$$

The exact solution and the curve resulting from the second order approximation in $1/n$ can be seen in Figure 6.3.

In Figure 6.4 we plot the dependence on the continuous variable n_2 , in the $n_1 \rightarrow \infty$ limit, of the area of the cross section of the horizon A_+ and the surface gravity κ_+ in the partner Lorentzian solutions.

In Appendix D the reader will find a translation of some of the numerical values above to SI units.

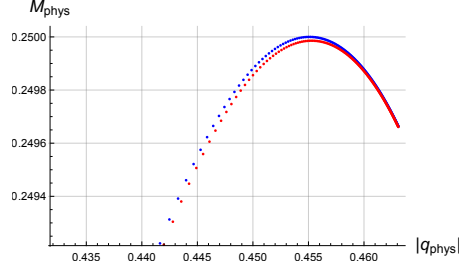


Figure 6.3: Correlation plot in the $(|q_{\text{phys}}|, M_{\text{phys}})$ plane in the limit $n_1 \rightarrow \infty$. The red points lie on the curve (6.25), the blue dots arise from the exact solutions (6.12) and (6.14).

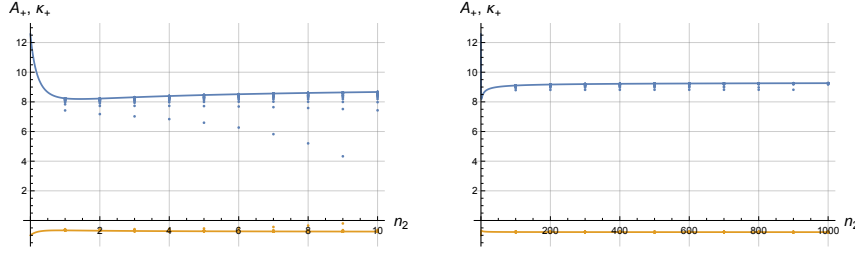


Figure 6.4: Plots of A_+ (blue line) and κ_+ (orange line) as functions of a continuous variable $n_2 \in [0, 10]$ (left plot) and $n_2 \in [0, 1000]$ (right plot). The dots correspond to the values obtained for the solutions with the given values of n_2 and with n_1 increasing in logarithmic steps to 10000 (left plot) and 100000 (right plot).

7 Dirac strings

Similarly to [5], the existence of charged spinor fields on the Euclidean manifold leads to further constraints on the parameters of the solution. Indeed, comparing (3.18) with (3.20) shows that the transition from a gauge potential which is regular near $\{\cos(\theta) = 1, r = r_i\}$ to a gauge potential which is regular near $\{\cos(\theta) = -1, r = r_i\}$ requires a gauge transformation

$$A \mapsto A + \frac{2p}{\Xi} \left(d\varphi - \frac{a}{a^2 - r_i^2} dt \right).$$

If a Dirac field ψ carries a charge q_0 , such a gauge transformation induces a transformation

$$\psi \mapsto \exp \left(\frac{2iq_0p}{\hbar\Xi} \left(\varphi - \frac{a}{a^2 - r_i^2} t \right) \right) \psi.$$

Recall that φ is $2\pi/k$ -periodic, with $k = 1$ except in the Page limit where $k = 2$ can arise and which needs to be analysed separately in any case, see Section E.3 below. Thus in the remainder of this section we assume that φ is 2π periodic. The requirement of single-valuedness of ψ results in the condition

$$\frac{2q_0p}{\hbar\Xi} =: \hat{n}_1 \in \mathbb{Z}. \quad (7.1)$$

Next, (3.18) and (3.21) show that the gauge potentials

$$A + \frac{p}{\Xi} \left(d\varphi - \frac{a}{a^2 - r_i^2} dt \right) - \frac{er_i}{\Xi(a^2 - r_i^2)} dt, \quad i = 1, 2, \quad (7.2)$$

are regular near $r = r_i$ and $\theta = 0$. Passing from one to the other requires a gauge transformation

$$A \mapsto A + \left(\frac{pa + er_2}{\Xi(a^2 - r_2^2)} - \frac{pa + er_1}{\Xi(a^2 - r_1^2)} \right) dt.$$

Keeping in mind that t has period $2\pi\omega$, the associated transformation of the spinor field ψ leads to the further condition

$$\underbrace{\frac{q_0}{\hbar\Xi}}_{\hat{n}_1/2} \left(\underbrace{p \left(\frac{a\omega}{r_1^2 - a^2} - \frac{a\omega}{r_2^2 - a^2} \right)}_{n_1} + e\omega \left(\frac{r_1}{r_1^2 - a^2} - \frac{r_2}{r_2^2 - a^2} \right) \right) \in \mathbb{Z}^*. \quad (7.3)$$

A similar analysis near $\theta = \pi$ leads to the further condition

$$\underbrace{\frac{q_0}{\hbar\Xi}}_{\hat{n}_1/2} \left(\underbrace{p \left(\frac{a\omega}{r_1^2 - a^2} - \frac{a\omega}{r_2^2 - a^2} \right)}_{n_1} - e\omega \left(\frac{r_1}{r_1^2 - a^2} - \frac{r_2}{r_2^2 - a^2} \right) \right) \in \mathbb{Z}^*. \quad (7.4)$$

We conclude that we must have

$$\frac{\hat{n}_1(n_1 - n_2)}{2} \in \mathbb{N}^*, \quad (7.5)$$

and that there exists $\hat{n}_2 \in \mathbb{N}^*$ so that

$$e\omega \left(\frac{r_1}{r_1^2 - a^2} - \frac{r_2}{r_2^2 - a^2} \right) = \hat{n}_2. \quad (7.6)$$

Eliminating q_0 between (7.1) and (7.3) imposes a quantised relation between p and e :

$$p = \underbrace{\frac{\omega}{2} \left(\frac{r_1}{r_1^2 - a^2} - \frac{r_2}{r_2^2 - a^2} \right)}_{=: \sigma} \times \frac{\hat{n}_1}{\hat{n}_2} \times e. \quad (7.7)$$

Recall that given a set (M, a, p_{eff}^2) , parameterised by two integers (n_1, n_2) with $n_1 < n_2$ and arising from a smooth compact Riemannian solution, we have so far been associating to it a Lorentzian partner solution with the same values of M and a , with $p^2 = p_{\text{eff}}^2$ and with $e = 0$. However, if one adds the requirement of well-defined charges spinor fields to the picture, instead of choosing $e = 0$ on the Lorentzian side one might wish to request that (7.7) holds. This adds two further quantum numbers (\hat{n}_1, \hat{n}_2) to the picture. Taking into account the inequality $p_{\text{eff}}^2 = p^2 - e^2 > 0$ one is led to the condition

$$\sigma \frac{\hat{n}_1}{\hat{n}_2} > 1. \quad (7.8)$$

Given a pair (\hat{n}_1, \hat{n}_2) such that (7.8) holds (note that this can always be achieved by choosing \hat{n}_1 large enough), we can determine $|q_0|$, $|e|$ and $|p|$ from (7.1)-(7.7):

$$|e| = \sqrt{\frac{p_{\text{eff}}^2}{(\sigma \frac{\hat{n}_1}{\hat{n}_2})^2 - 1}}, \quad |p| = \sigma \frac{\hat{n}_1}{\hat{n}_2} \sqrt{\frac{p_{\text{eff}}^2}{(\sigma \frac{\hat{n}_1}{\hat{n}_2})^2 - 1}}, \quad |q_0| = \frac{\hbar\Xi}{2} \sqrt{\frac{\sigma^2 \hat{n}_1^2 - \hat{n}_2^2}{p_{\text{eff}}^2}}.$$

In this way we are led to a discrete family of solutions parameterised by four integers $(n_1, n_2, \hat{n}_1, \hat{n}_2)$ subject to the constraints (7.5) and (7.8).

It holds that $p_{\text{eff}}^2 < p^2 \rightarrow (\hat{n}_1/\hat{n}_2) \rightarrow \infty p_{\text{eff}}^2$, $e \rightarrow (\hat{n}_1/\hat{n}_2) \rightarrow \infty 0$, and thus $p_{\text{eff}}^2 < p^2 + e^2 \rightarrow (\hat{n}_1/\hat{n}_2) \rightarrow \infty p_{\text{eff}}^2$.

The global structure of the resulting Lorentzian partners is the same as in the case $e = 0$, see Figure B.1.

A A typical solution

We rescale the metric so that $\lambda = 1$. We choose $n_1 = 10$, $n_2 = 9$. With this choice the system (5.3-5.7) takes the explicit form

$$\begin{aligned} -a^2 + p_{\text{eff}}^2 - 2Mr_1 + r_1^2 + a^2 r_1^2 - r_1^4 &= 0, \\ -2a + 2a^3 - 20M + 20r_1 + 20a^2 r_1 - 40r_1^3 &= 0, \\ -2a + 2a^3 + 18M - 18r_2 - 18a^2 r_2 + 36r_2^3 &= 0, \\ 10(r_1^2 - a^2) - 9(r_2^2 - a^2) &= 0, \end{aligned} \quad (\text{A.1})$$

as well as an equation for r_2 identical to the first equation above. The Buchberger algorithm for finding a Gröbner basis for Eq.(A.1), as implemented in MATHEMATICA, yields the following system

$$\begin{aligned} &141447860388864000000(p_{\text{eff}}^2)^2 - 2530102285619187840000(p_{\text{eff}}^2)^3 + 6902836371659336516100(p_{\text{eff}}^2)^4 \\ &\quad - 7443462023036715884580(p_{\text{eff}}^2)^5 + 3324944139689702617201(p_{\text{eff}}^2)^6 = 0, \\ &269121969463191443505728626849880910201000(p_{\text{eff}}^2)^2 + 5123491133454465890342571180870383758599000a^2(p_{\text{eff}}^2)^2 \\ &\quad - 4306620505226193997812468562360852027723500(p_{\text{eff}}^2)^3 + 661016788713267074222610725116146960042870(p_{\text{eff}}^2)^4 \\ &\quad - 1418820167927814403912453122762613275222257(p_{\text{eff}}^2)^5 = 0, \\ &1840946142733449839332390348051522429788563882649600000M(p_{\text{eff}}^2) \\ &\quad - 140403030498229867043777134104718536116027658797039040000a(p_{\text{eff}}^2)^2 \\ &\quad + 425794621585557982844978758649217892223137640430823652700a(p_{\text{eff}}^2)^3 \\ &\quad - 476718734408676529956326149018521215355879124052827578300a(p_{\text{eff}}^2)^4 \\ &\quad + 216318197798255246294998226248424687617679013902862944743a(p_{\text{eff}}^2)^5 = 0, \\ &10604338062917514381295873956265388153861661532099121130946560000000a^3 \\ &\quad - 10604338062917514381295873956265388153861661532099121130946560000000a^5 \\ &\quad + 17673896771529190635493123260442313589769435886831868551577600000000a(p_{\text{eff}}^2) \\ &\quad - 58822730414627718291223364304260174172128286418763128059980799680000a(p_{\text{eff}}^2)^2 \\ &\quad + 1755642879359412179543337165217487045071628171531789605489627506273900a(p_{\text{eff}}^2)^3 \\ &\quad - 195450260281041300968034654172581067701751874639137635441883692255820a(p_{\text{eff}}^2)^4 \\ &\quad + 893243009923318159877420930128536388883746991239505692176977591346539a(p_{\text{eff}}^2)^5 \\ &\quad + 3534779354305838127098624652088462717953887177366373710315520000000(p_{\text{eff}}^2)r_2 = 0, \end{aligned} \quad (\text{A.2})$$

together with an identical equation for r_1 .

The structure of the equations is typical in the following sense: Since MATHEMATICA does not manage to find a Gröbner basis when n_1 and n_2 are left as general parameters, our procedure is to provide the values of n_1 and n_2 and then seek the basis. All the resulting polynomials that we have inspected have then a structure identical to the one above.

It can be seen that solving the system (A.2) in the manner described above requires only solving polynomial equations in a single variable of at most forth

order, and so explicit analytic expressions can be given. However, the expressions obtained, especially for r_1 and r_2 , become very unwieldy. Therefore, instead of the full analytic expressions, we give only the first five nontrivial digits after the decimal point of the parameters for the solution of (A.1) that fulfills the constraints:

$$r_1 = 0.48613, \quad r_2 = 0.51203, \quad M = 0.25211, \quad a = 0.060481, \quad p_{\text{eff}}^2 = 0.067439. \quad (\text{A.3})$$

B Physical quantities

B.1 Euclidean case

The “surface gravity” of the zeros of the ∂_t -Killing vector, located at r_1 and r_2 , reads

$$\kappa := \frac{1}{2\Xi(r_i^2 - a^2)} \Delta'_r|_{r=r_i} = -\frac{1}{2\Xi(r_i^2 - a^2)} \Delta'_r|_{r=r_2}. \quad (\text{B.1})$$

Since ∂_φ and ∂_t are Killing fields and

$$(t, r, \theta, \varphi) \in [0, \frac{2\pi}{\kappa}) \times [r_1, r_2) \times [0, \pi) \times [0, 2\pi),$$

we obtain the following formula for the areas of the zero-set of ∂_t , located at r_1 and r_2 ,

$$\begin{aligned} A_i &= 2\pi \int_0^\pi \sqrt{g_{\varphi\varphi} g_{\theta\theta}}|_{r=r_i} d\theta = \pi \int_0^\pi \frac{(r_i^2 - a^2) \sin(\theta)}{\Xi} d\theta \\ &= \frac{4\pi(r_i^2 - a^2)}{\Xi} \end{aligned} \quad (\text{B.2})$$

and for the volume of the manifold

$$\begin{aligned} V &= 2\pi \frac{2\pi}{\kappa} \int_{r_1}^{r_2} \int_0^\pi \sqrt{g} d\theta dr = \frac{4\pi^2}{\kappa} \int_{r_1}^{r_2} \int_0^\pi \frac{\Sigma \sin(\theta)}{\Xi^2} d\theta dr \\ &= \frac{8\pi^2}{3\kappa\Xi^2} [(r_2^3 - r_1^3) - a^2(r_2 - r_1)]. \end{aligned} \quad (\text{B.3})$$

The action of the Einstein-Maxwell system is given by

$$\begin{aligned} S &= -\frac{1}{16\pi} \int (R - 2\Lambda - F^2) \sqrt{g} d^4x \\ &= \underbrace{-\frac{1}{16\pi} \int (R - 2\Lambda) \sqrt{g} d^4x}_{:= S_G} + \underbrace{\frac{1}{16\pi} \int F^2 \sqrt{g} d^4x}_{:= S_{\text{EM}}}. \end{aligned} \quad (\text{B.4})$$

Let S_G be the gravitational action, we have

$$\begin{aligned} S_G &= -\frac{1}{16\pi} \int (R - 2\Lambda) \sqrt{g} d^4x \\ &= -\frac{\Lambda}{8\pi} V \\ &= -\Lambda \frac{\pi}{3\kappa\Xi^2} [(r_2^3 - r_1^3) - a^2(r_2 - r_1)]. \end{aligned} \quad (\text{B.5})$$

A MATHEMATICA calculation gives

$$F^2 := g^{\alpha\beta} g^{\mu\nu} F_{\alpha\mu} F_{\beta\nu} = \frac{(e-p)^2}{(a \cos(\theta) + r)^4} + \frac{(e+p)^2}{(r - a \cos(\theta))^4}, \quad (\text{B.6})$$

leading to

$$\begin{aligned} S_{\text{EM}} &= \frac{1}{16\pi} \int F^2 \sqrt{g} d^4 x \\ &= \frac{1}{16\pi} \frac{4\pi^2}{\kappa} \int_{r_1}^{r_2} \int_0^\pi F^2 \sqrt{g} d\theta dr \\ &= \frac{\pi(p^2 + e^2)}{\kappa \Xi^2} \left(\frac{r_1}{r_1^2 - a^2} - \frac{r_2}{r_2^2 - a^2} \right). \end{aligned} \quad (\text{B.7})$$

Together this yields

$$S = \frac{\pi}{\kappa \Xi^2} \left\{ -\frac{\Lambda}{3} [(r_2^3 - r_1^3) - a^2(r_2 - r_1)] + (e^2 + p^2) \left(\frac{r_1}{r_1^2 - a^2} - \frac{r_2}{r_2^2 - a^2} \right) \right\}. \quad (\text{B.8})$$

The minimum of the action is attained at $(n_1, n_2) = (2, 1)$, and equals $S_{\min} \approx -2.357$. Since $r_1 \rightarrow_{n_1 \rightarrow \infty} a$ and $p_{\text{eff}}^2 \rightarrow_{n_1 \rightarrow \infty} 0.32$ (see (6.11)), the action is unbounded from above. It follows from the analysis in Section 6 that S_G is bounded from above by $-\pi/2$, so only the Maxwell action grows without bound. Now, if r_2 is close to r_1 , then the Maxwell action is very small. One expects this to be true when both n_1 and n_2 are very large. This suggests very strongly that the set of pairs (n_1, n_2) , for which the Maxwell action S_{EM} is very small compared to the gravitational one, is unbounded. Numerics shows that this is indeed the case for all large numbers n_1 that we have looked at.

In particular solutions with very large values of $n_1 - n_2$ are strongly suppressed when path-integral arguments are invoked.

B.2 Lorentzian case

In this section we consider the *Lorentzian solutions with $e = 0$ and with the value of a , M and p_{eff}^2 arising from a smooth compact Euclidean solution with $e = 0$* . To avoid ambiguities, we write

$$\Delta_{\text{Lor}} := (r^2 + a^2)(1 - \lambda r^2) - 2Mr + p^2 + e^2 \quad \text{and} \quad \Xi_{\text{Lor}} := 1 + \lambda a^2. \quad (\text{B.9})$$

In all solutions that we have found the function Δ_{Lor} has precisely two real first-order zeros, with exactly one positive, denoted by r_+ . The associated horizon is usually referred to as the *cosmological horizon*. The global structure of the Lorentzian solution is shown in Figure B.1.

As already pointed-out, there is an ambiguity in the definition of total mass of the associated Lorentzian space-time. In a Hamiltonian approach this ambiguity is related to the choice of the Killing vector field for which we calculate the Hamiltonian [3]. In any case, the physical mass M_{phys} and the angular momentum J_{phys} are usually calculated using the formulae

$$M_{\text{phys}} = \frac{M}{\Xi_{\text{Lor}}^2}, \quad J_{\text{phys}} = \frac{aM}{\Xi_{\text{Lor}}^2}. \quad (\text{B.10})$$

(The above mass of the Lorentzian solution is obtained by calculating the Hamiltonian associated with the Killing vector field $\Xi_{\text{Lor}} \partial_t + 3^{-1} \Lambda a \partial_\varphi$, while the total angular momentum is the Hamiltonian associated with ∂_φ .)

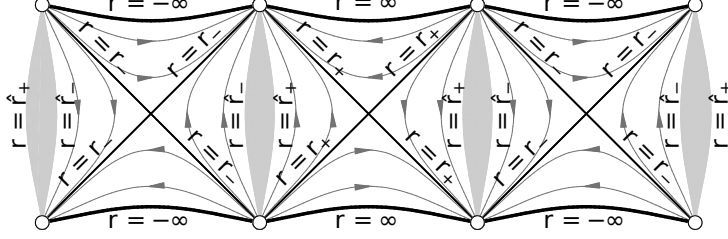


Figure B.1: A projection diagram for the Kerr-Newman - de Sitter metrics with exactly two distinct real first-order zeros of Δ_r , $r_- < 0 < r_+$, from [4]. Outside of the shaded regions, which contain the singular rings and the time-machines with boundaries at \hat{r}_\pm , the diagram represents accurately (within the limitations of a two-dimensional projection) the global structure of the space-time. Here r_- and r_+ indicate the radii of the Lorentzian horizons, not to be confused with the Euclidean rotation axes from the body of the paper.

The area of the cross-section of the horizon located at r_+ is given by

$$A_+ = \frac{4\pi(r_+^2 + a^2)}{\Xi_{\text{Lor}}}, \quad (\text{B.11})$$

and is usually interpreted as the entropy of the cosmological horizon [7]. The surface gravity of the horizon $r = r_+$ associated with the Killing vector $X := \partial_t + \Omega \partial_\varphi$, where Ω is chosen so that X is tangent to the generators of the horizon, is

$$\kappa_+ = \frac{1}{2\Xi_{\text{Lor}}(r_+^2 + a^2)} \Delta'_{\text{Lor}}|_{r=r_+}. \quad (\text{B.12})$$

C A sample

We list in Table C.1 the defining parameters of all solutions for $\lambda = 1$, $\zeta = -1$, $n_1, n_2 \in \{-10, 10\}$, $n_1 > n_2$, fulfilling the constraints, as well as some associated physical quantities. The constraints $a < r_1 < r_2$ and $a^2 < 1$ are clearly seen to be fulfilled. The physical quantities M_{phys} , $|J_{\text{phys}}|$, $|q_{\text{phys}}|$ are defined in (B.10), while S denotes the Euclidean action of the solutions.

D SI units

Recall that $\lambda := \Lambda/3$. The replacements

$$r \mapsto \sqrt{\frac{1}{\lambda}} \times r, \quad M \mapsto \sqrt{\frac{1}{\lambda}} \times M, \quad a \mapsto \sqrt{\frac{1}{\lambda}} \times a, \quad e \mapsto \sqrt{\frac{1}{\lambda}} \times e, \quad (\text{D.1})$$

yield

$$\Delta_r \mapsto \frac{1}{\lambda} \underbrace{\left((r^2 + a^2)(1 - r^2) - 2Mr + p_{\text{eff}}^2 \right)}_{:= \Delta_r^{\lambda=1}}, \quad \Delta'_r \mapsto \frac{1}{\sqrt{\lambda}} \Delta_r^{\lambda=1}, \quad \Xi \mapsto \underbrace{1 - a^2}_{:= \Xi^{\lambda=1}}.$$

n_1	n_2	$n_1 - n_2$	a	r_1	r_2	M	p_{eff}^2	M_{phys}	$ J_{\text{phys}} $	$ q_{\text{phys}} $	S_G	S
2	1	1	0.05720	0.4147	0.5837	0.2449	0.06344	0.2433	0.01392	0.2511	-2.368	-2.357
3	1	2	0.09837	0.3698	0.6253	0.2398	0.06764	0.2352	0.02314	0.2576	-2.377	-2.335
3	2	1	0.05939	0.4494	0.5488	0.2497	0.06610	0.2480	0.01473	0.2562	-2.353	-2.340
4	1	3	0.1264	0.3426	0.6493	0.2366	0.07260	0.2292	0.02898	0.2652	-2.380	-2.291
4	2	2	0.1063	0.4159	0.5785	0.2504	0.07462	0.2449	0.02604	0.2701	-2.341	-2.290
4	3	1	0.05997	0.4638	0.5344	0.2510	0.06681	0.2492	0.01494	0.2576	-2.349	-2.336
5	1	4	0.1460	0.3247	0.6646	0.2346	0.07709	0.2249	0.03284	0.2718	-2.380	-2.233
5	2	3	0.1403	0.3930	0.5971	0.2518	0.08399	0.2422	0.03398	0.2842	-2.326	-2.211
5	3	2	0.1088	0.4370	0.5571	0.2538	0.07688	0.2479	0.02698	0.2740	-2.330	-2.276
5	4	1	0.06020	0.4717	0.5265	0.2515	0.06710	0.2497	0.01503	0.2581	-2.347	-2.334
6	1	5	0.1602	0.3120	0.6751	0.2333	0.08086	0.2217	0.03553	0.2772	-2.380	-2.165
6	2	4	0.1648	0.3768	0.6096	0.2533	0.09238	0.2401	0.03957	0.2959	-2.312	-2.110
6	3	3	0.1452	0.4173	0.5721	0.2571	0.08814	0.2466	0.03580	0.2908	-2.308	-2.182
6	4	2	0.1100	0.4492	0.5447	0.2552	0.07789	0.2492	0.02740	0.2758	-2.325	-2.270
6	5	1	0.06032	0.4767	0.5215	0.2518	0.06724	0.2499	0.01508	0.2584	-2.346	-2.333

Table C.1: Some selected solutions with the most relevant physical parameters in dimensionless units

(D.2)

It is easy to check that if

$$\left(r_1^{\lambda=1}, r_2^{\lambda=1}, M^{\lambda=1}, a^{\lambda=1}, (p_{\text{eff}}^2)^{\lambda=1} \right)$$

is a solution of the system Eq.(5.3-5.7) for $\lambda = 1$, then

$$\begin{aligned} r_1 &= \sqrt{\frac{1}{\lambda}} \times r_1^{\lambda=1}, \quad r_2 = \sqrt{\frac{1}{\lambda}} \times r_2^{\lambda=1}, \quad M = \sqrt{\frac{1}{\lambda}} \times M^{\lambda=1}, \\ a &= \sqrt{\frac{1}{\lambda}} \times a^{\lambda=1}, \quad p_{\text{eff}}^2 = \frac{1}{\lambda} \times (p_{\text{eff}}^2)^{\lambda=1}, \end{aligned} \quad (\text{D.3})$$

provides a solution of this system with an arbitrary value λ .

In SI-units we have

$$M_{\text{phys}}^{SI} = \frac{c^2}{G} \times M_{\text{phys}}, \quad |q_{\text{phys}}|^{SI} = \sqrt{\frac{4\pi\epsilon_0 c^4}{G}} \times |q_{\text{phys}}|, \quad (\text{D.4})$$

where G is the gravitational constant, c the speed of light and ϵ_0 the electric constant. Then the physical angular momentum in SI-units can be computed as

$$J_{\text{phys}}^{SI} = a \times c \times M_{\text{phys}}^{SI}. \quad (\text{D.5})$$

Putting all this together we obtain

$$M_{\text{phys}}^{SI} = \frac{c^2}{G} \times \frac{1}{\Xi_{\text{Lor}}^2} \times \sqrt{\frac{1}{\lambda}} \times M^{\lambda=1}, \quad (\text{D.6})$$

$$a^{SI} = \sqrt{\frac{1}{\lambda}} \times a^{\lambda=1}, \quad (\text{D.7})$$

$$|q_{\text{phys}}|^{SI} = \sqrt{\frac{4\pi\epsilon_0 c^4}{G} \times \frac{1}{\lambda} \times \frac{1}{\Xi_{\text{Lor}}^2} \times (p_{\text{eff}}^2)^{\lambda=1}}, \quad (\text{D.8})$$

$$J_{\text{phys}}^{SI} = c \times a^{SI} \times M_{\text{phys}}^{SI}. \quad (\text{D.9})$$

Since Ξ_{Lor} and Δ_{Lor} are invariant under rescaling, it follows

$$A_+^{SI} = \frac{1}{\lambda} A_+^{\lambda=1}, \quad (\text{D.10})$$

$$\kappa_+^{SI} = c^2 \sqrt{\lambda} \kappa_+^{\lambda=1}. \quad (\text{D.11})$$

The black hole temperature in SI-units T^{SI} reads

$$T_{kg^{-1}} = \frac{1}{2\pi} \frac{G}{c^2} \sqrt{\lambda} \times \kappa_+^{\lambda=1}, \quad (\text{D.12})$$

$$T^{SI} = \frac{c^3 \hbar}{k G} \times T_{kg^{-1}}, \quad (\text{D.13})$$

where $\hbar = 1.054 \times 10^{-34} \text{ Js}$ and $k = 1.38 \times 10^{-23} \text{ JK}^{-1}$ are the reduced Planck's constant and the Boltzmann constant respectively. Table D.1 lists some values of M_{phys} in units of the mass of Milky Way, taken to be $10^{12} M_{\odot}$,

$$M_{\text{phys}} = M_{\text{astro}} \times 10^{12} M_{\odot} \sqrt{\frac{\Lambda}{\Lambda_0}},$$

where M_{\odot} is the mass of the sun and

$$\Lambda_0 = 3H_0^2 \Omega_{\Lambda} = 1.11 \times 10^{-52} m^{-2}$$

is the value of the cosmological constant as resulting from the Planck observations [1] (compare [?, 12, 17]). We moreover use $G = 6.67 \times 10^{-11} \frac{m^3}{kg s^2}$, $c = 299 \times 10^8 \frac{m}{s}$, and $\epsilon_0 = 8.85 \times 10^{-12} m^{-3} kg^{-1} s^4 A^2$, $M_{\odot} = 1.99 \times 10^{30} kg$.

$M_{\text{phys}}/10^{10} M_{\text{Milky Way}}$	type
2.27	minimum
2.84	maximum
2.71	at minimal charge
2.77	at maximal charge

Table D.1: Some cosmological values of M_{phys} , in Milky Way mass units.

Another set of amusing questions is, which values of Λ are required to obtain the charge e^- of an electron as minimal value for the physical charge $|q_{\text{phys}}|^{SI} = e^-$, or the mass of an electron M_e , or of a proton M_p , as minimal value of the physical mass:

$$e^- = 1.60 \times 10^{-19} C, \quad M_e = 9.11 \times 10^{-31} kg, \quad M_p = 1.67 \times 10^{-27} kg.$$

The results are given in Table D.2.

E Lorentzian partner solutions

Consider a set of parameters n_1, n_2, M, a , and p_{eff}^2 that solve, together with the positive zeros of Δ_r , the system (5.3-5.7) and fulfill the constraints. For this set of parameters we calculate the zeros of the Lorentzian partner Δ_{Lor} given by (B.9) of the Euclidean function Δ_r . As already mentioned, for all (n_1, n_2) that we have investigated the function Δ_{Lor} has only two real first-order zeros, with exactly one positive zero r_+ .

minimal physical mass /charge	Λ / m^{-2}	Λ / Λ_0
e^-	9.92×10^{70}	8.94×10^{122}
M_e	2.72×10^{113}	2.45×10^{165}
M_p	8.06×10^{106}	7.26×10^{158}

Table D.2: Values of Λ required to obtain e^- as minimal physical charge and M_e/M_p as minimal physical mass. Λ_0 is the current estimate of the value of the cosmological constant.

E.1 Geometric units

In Table E.1 we list the values of r_+ , the surface gravity (“temperature”) and the area (“entropy”) of the horizon.

n_1	n_2	$n_1 - n_2$	r_+	κ_+	A_+
2	1	1	0.612	-0.246	4.730
3	1	2	0.667	-0.377	5.663
3	2	1	0.594	-0.216	4.467
4	1	3	0.699	-0.452	6.239
4	2	2	0.649	-0.355	5.368
4	3	1	0.589	-0.208	4.394
5	1	4	0.719	-0.498	6.617
5	2	3	0.682	-0.439	5.967
5	3	2	0.643	-0.349	5.282
5	4	1	0.587	-0.204	4.364
6	1	5	0.732	-0.529	6.880
6	2	4	0.703	-0.493	6.376
6	3	3	0.676	-0.438	5.890
6	4	2	0.641	-0.346	5.244
6	5	1	0.586	-0.203	4.349

Table E.1: The surface gravity and area for some selected solutions, with $\Lambda = 3$.

E.2 SI units, $\Lambda = 1.11 \times 10^{-52} m^{-2}$

With the formulae given in Appendix D we can calculate the interesting physical quantities in SI-units for the measured cosmological value Λ_0 of Λ from the data for $\Lambda = 3$. Using the Planck mission data $\Omega_\Lambda = 0.6911$ and $H_0 = 67.74 km/(s Mpc)$, (see [17], p. 31, TT, TE, EE + lowP + lensing), the cosmological constant can be calculated to be

$$\Lambda_0 c^2 = 3 H_0^2 \Omega_\Lambda = 9.99 \times 10^{-36} s^{-2} \Rightarrow \Lambda_0 = 1.11 \times 10^{-52} m^{-2}$$

The reader will find some physical quantities of interest associated with our solutions in Tables E.2 and E.3.

To close this section, let us assume that the above universe consists of protons, neutrons, and hydrogen atoms. This means that for the range of values, as given above, we have $n_{\text{items}} \approx M_{\text{phys}}/M_{\text{proton}} \approx 2 \times 10^{79}$ items. On the other hand $n_{\text{protons}} = |q_{\text{phys}}|/e^- \approx 2 \times 10^{61}$ particles are required to produce the required charge. As a consequence, every 10^{18} -th item carries a charge.

n_1	n_2	$n_1 - n_2$	$r_+/10^{26} m$	$M_{phys}/10^{52} kg$	$ J_{phys} /10^{86} kg m^2 s^{-1}$	$ q_{phys} /10^{42} C$	$ k_+ /10^{-10} ms^{-2}$	$A_+/10^{53} m^2$	$T/10^{-30} K$
2	1	1	1.006	5.387	1.519	4.790	1.345	1.278	0.545
3	1	2	1.097	5.207	2.524	4.914	2.062	1.530	0.836
3	2	1	0.977	5.490	1.607	4.888	1.181	1.207	0.479
4	1	3	1.149	5.074	3.162	5.060	2.470	1.686	1.001
4	2	2	1.066	5.421	2.841	5.153	1.938	1.451	0.786
4	3	1	0.969	5.517	1.631	4.914	1.136	1.188	0.461
5	1	4	1.181	4.978	3.583	5.186	2.723	1.788	1.104
5	2	3	1.120	5.362	3.708	5.422	2.401	1.613	0.974
5	3	2	1.057	5.487	2.944	5.228	1.906	1.427	0.773
5	4	1	0.966	5.528	1.640	4.924	1.117	1.179	0.453
6	1	5	1.203	4.909	3.877	5.289	2.891	1.859	1.172
6	2	4	1.156	5.316	4.318	5.645	2.696	1.723	1.093
6	3	3	1.112	5.459	3.906	5.547	2.393	1.592	0.970
6	4	2	1.053	5.517	2.990	5.261	1.893	1.417	0.768
6	5	1	0.964	5.534	1.645	4.929	1.108	1.175	0.449

Table E.2: Some physical quantities in SI units for selected solutions

n_1	2	3	3	4	4	4	5	5	5	5	6	6	6	6	6
n_2	1	1	2	1	2	3	1	2	3	4	1	2	3	4	5
$\frac{M_{phys}}{M_\odot}/10^{22}$	2.708	2.618	2.760	2.551	2.726	2.774	2.503	2.696	2.759	2.779	2.468	2.672	2.745	2.774	2.782
$= \frac{M_{phys}}{M_{gal}}/10^{10}$															

Table E.3: The physical mass in solar mass- and galaxy mass units for some selected solutions

F Page limit

The aim of this appendix is to discuss the charged solutions obtained by Page's limiting procedure [16]. (These solutions have been already been discussed in [13, Section 7.4, Equations (135)-(136)] from a rather different perspective; compare [14].) Recall that Page's approach is the following: Let r_0 be a zero of Δ_r , and let ϵ be a small parameter. We define new coordinates $(\chi, \bar{\varphi}, \eta)$ as

$$r = r_0 - \epsilon \cos(\chi), \quad (F1)$$

$$\varphi = \bar{\varphi} - \frac{a}{r_0^2 - a^2} t, \quad (F2)$$

$$t = \frac{\omega_0 \eta}{\epsilon}, \quad (F3)$$

where η and $\bar{\varphi}$ are 2π -periodic, and ω_0 is a constant to be determined. We choose the parameters (M, a, p_{eff}^2) so that

$$\Delta_r = C(1 - \cos^2(\chi))\epsilon^2 + O(\epsilon^3), \quad (F4)$$

for a suitable constant $C = C(\epsilon)$. After taking the limit $\epsilon \rightarrow 0$ the metric takes the form

$$ds^2 = 3(r_0^2 - a^2 \cos^2(\theta)) \times \left\{ \frac{1}{6\Lambda r_0^2 - a^2 \Lambda - 3} \left(d\chi^2 + \frac{(6\Lambda r_0^2 - a^2 \Lambda - 3)^2 \omega_0^2}{(r_0^2 - a^2)^2 (3 - a^2 \Lambda)^2} \sin^2(\chi) d\eta^2 \right) \right\} \quad (F5)$$

$$+ \frac{1}{3 - a^2 \Lambda \cos^2(\theta)} \left[d\theta^2 + \frac{(r_0^2 - a^2)^2 (3 - a^2 \Lambda \cos^2(\theta))^2}{(3 - a^2 \Lambda)^2 (r_0^2 - a^2 \cos^2(\theta))^2} \sin^2(\theta) \times \right. \\ \left. \left(d\bar{\varphi} + \frac{2ar_0\omega_0}{(r_0^2 - a^2)^2} \cos(\chi) d\eta \right)^2 \right] \Bigg\}. \quad (\text{E6})$$

An Euclidean signature will be obtained if

$$a^2 < r_0^2, \quad \Lambda a^2 < 3, \quad 6\Lambda r_0^2 - a^2 \Lambda - 3 > 0. \quad (\text{E7})$$

Note that the transformation $\eta \mapsto -\eta$ has the effect of changing the sign of ar_0 , so without loss of generality we can assume that $ar_0 > 0$. Since a simultaneous change of sign of a and r_0 leaves the metric invariant, we can assume that

$$a \geq 0 \text{ and } r_0 > 0.$$

Near $\chi = 0$ we introduce a new coordinate ϕ , 2π -periodic, chosen so that $g_{\eta\eta}|_{\chi=0} = 0$:

$$d\phi := \alpha \left(d\bar{\varphi} + \frac{2ar_0\omega_0}{(r_0^2 - a^2)^2} d\eta \right), \quad (\text{E8})$$

for some constant $\alpha \in \mathbb{R}^*$. Standard considerations show that the metric will be smooth if

$$\omega_0^2 \frac{(6\Lambda r_0^2 - a^2 \Lambda - 3)^2}{(r_0^2 - a^2)^2 (3 - a^2 \Lambda)^2} = 1 \quad \Longleftrightarrow \quad \omega_0 = \pm \underbrace{\frac{(r_0^2 - a^2)(3 - a^2 \Lambda)}{6\Lambda r_0^2 - a^2 \Lambda - 3}}_{=: \omega_P > 0}, \quad (\text{E9})$$

$$\alpha^2 \frac{(r_0^2 - a^2)^2 (a^2 \Lambda \cos^2(\theta) - 3)^2}{(3 - a^2 \Lambda)^2 (r_0^2 - a^2 \cos^2(\theta))^2} \Big|_{\Theta=0} = 1 \quad \Longleftrightarrow \quad \alpha = \pm 1. \quad (\text{E10})$$

(The constant ω_P of (E.9) coincides with Page's constant ω_{Page} ,

$$\omega_{\text{Page}} = \frac{r_0^2(3 - a^2 \Lambda)(r_0^2 - a^2)}{3(a^2 + \Lambda r_0^4)}, \quad (\text{E11})$$

when $p_{\text{eff}}^2 = 0$ and when the requirement that r_0 is a double zero of Δ , which is implicit in the construction here, is taken into account.)

When $a = 0$, the metric is now a product of two round metrics, with possibly different curvatures, on $S^2 \times S^2$. From now on we only consider the case

$$a > 0.$$

Near $\chi = \pi$ we introduce a new angular coordinate $\hat{\phi}$, 2π -periodic, chosen so that $g_{\eta\eta}|_{\chi=\pi} = 0$:

$$d\hat{\phi} := \hat{\alpha} \left(d\bar{\varphi} - \frac{2ar_0\omega_0}{(r_0^2 - a^2)^2} d\eta \right). \quad (\text{E12})$$

One checks that smoothness of the metric there is already guaranteed by (E9)-(E10).

Eliminating $d\bar{\varphi}$ between (E8) and (E12) we find

$$\hat{\alpha} d\hat{\phi} = \alpha d\phi - \frac{4ar_0\omega_0}{(r_0^2 - a^2)^2} d\eta, \quad (\text{E13})$$

Keeping in mind that η , ϕ and $\hat{\phi}$ are 2π -periodic, we are led to the condition

$$\frac{4ar_0\omega_0}{(r_0^2 - a^2)^2} =: n \in \mathbb{Z}^*. \quad (\text{E.14})$$

Equivalently,

$$\frac{4ar_0(3 - a^2\Lambda)}{(r_0^2 - a^2)(6\Lambda r_0^2 - a^2\Lambda - 3)} = |n| \in \mathbb{N}^*. \quad (\text{E.15})$$

To proceed, we prescribe $n \in \mathbb{Z}^*$, solve the system consisting of the equations $\Delta(r_0) = \Delta'(r_0)$ together with (E.15) for (r_0, a, M) , and check if the constraints are fulfilled.

E.1 Parametrization of r_0 and a by v and \bar{e}

One can provide an explicit parameterisation of solutions of the equations

$$\Delta_r(r_0, a, M, p_{\text{eff}}^2) = 0, \quad (\text{E.16})$$

$$\Delta'_r(r_0, a, M) = 0, \quad (\text{E.17})$$

which proceeds as follows: Solving (E.17) for M yields

$$M = \frac{1}{3}r_0(a^2\Lambda - 2\Lambda r_0^2 + 3). \quad (\text{E.18})$$

Using (E.18) in (E.16) and introducing $v \in (0, 1)$ and $\bar{e} \in \mathbb{R}$ through the equations

$$a = vr_0 \text{ and } p_{\text{eff}}^2 = \bar{e}r_0^2$$

(note that $r_0 \neq 0$ by (E.7), and that we allow now a negative $p_{\text{eff}}^2 = p^2 - e^2$) leads to

$$(1 - v^2) \left(1 - \frac{\Lambda r_0^2}{3} \right) - \frac{2}{3} (v^2 r_0^2 \Lambda - 2\Lambda r_0^2 + 3) + \bar{e} = 0. \quad (\text{E.19})$$

Solving (E.19) for r_0 , one is led to the condition

$$\bar{e} < 1 + v^2, \quad (\text{E.20})$$

together with

$$r_0 = \sqrt{\frac{3(v^2 + 1 - \bar{e})}{3 - v^2}} \frac{1}{\sqrt{\Lambda}}. \quad (\text{E.21})$$

(E.21) and $a = vr_0$ inserted in (E.18) give

$$M = \frac{(1 - v^2)^2 + \bar{e}(2 - v^2)}{3 - v^2} r_0. \quad (\text{E.22})$$

Using (E.21) and $a = vr_0$ in (E.15) yields

$$n = \frac{4v((\bar{e} - 2)v^2 - v^4 + 3)}{(1 - v^2)((\bar{e} + 6)v^2 - 6\bar{e} - v^4 + 3)}. \quad (\text{E.23})$$

This equation is invariant under the replacement $(n, v) \rightarrow (-n, -v)$. Hence, from now on we assume

$$n > 0.$$

The constraints (E.7) then become

$$0 < v < 1, \quad 0 < v^6 - (\bar{e} + 1)v^4 + 3(\bar{e} - 3)v^2 + 9, \quad 0 < (\bar{e} + 6)v^2 - 6\bar{e} - v^4 + 3. \quad (\text{E.24})$$

F.1.1 Magnetic charge equal to electric charge (possibly zero)

When $\bar{e} = 0$ the metric coincides with the Page metric, let us discuss this case for completeness. Equations (F23) and (F24) reduce to

$$n = \frac{4\nu(\nu^2 + 3)}{3 + 6\nu^2 - \nu^4}, \quad (\text{F25})$$

and

$$0 < \nu < 1, \quad 0 < \nu^6 - \nu^4 - 9\nu^2 + 9, \quad 0 < 6\nu^2 - \nu^4 + 3. \quad (\text{F26})$$

It follows easily, that if the first inequality in (F26) holds, the other two inequalities hold as well. A simple analysis of (F25) shows, that $0 < \nu < 1$ and $n \in \mathbb{N}^*$ imply $n = 1$. For this value of n , (F25) can be solved exactly. The only solution fulfilling $0 < \nu < 1$ is

$$\begin{aligned} \nu_{\text{Page}} &= -\sqrt{\sqrt[3]{1+\sqrt{2}} - \frac{1}{\sqrt[3]{1+\sqrt{2}}}} + 2 \\ &\quad + \frac{1}{2} \sqrt{-4\sqrt[3]{1+\sqrt{2}} + \frac{4}{\sqrt[3]{1+\sqrt{2}}} + \frac{32}{\sqrt{\sqrt[3]{1+\sqrt{2}} - \frac{1}{\sqrt[3]{1+\sqrt{2}}}} + 2}} + 16 - 1 \\ &\approx 0.2817. \end{aligned} \quad (\text{F27})$$

Using this value in (F21) and (F22) yields

$$r_0 = \frac{1.0529}{\sqrt{\Lambda}}, \quad a \approx \frac{0.2967}{\sqrt{\Lambda}}, \quad M \approx \frac{0.3056}{\sqrt{\Lambda}}. \quad (\text{F28})$$

We continue with the case $\bar{e} > 0$.

F.1.2 $\bar{e} > 0$

The addition of a positive charge parameter \bar{e} increases the right-hand side of the second inequality in (F24) $\forall \nu \in (0, 1)$. Thus from the analysis of the uncharged case, we can conclude that this constraint holds as well in the charged case.

The right-hand side of the third inequality in (F24) is monotonously increasing for $\nu \in (0, 1)$. It follows that the infimum and supremum are attained at $\nu = 0$ and $\nu = 1$ respectively. From this we can conclude the following:

- The inequality $\bar{e} < \frac{8}{5}$ is a necessary criterion to obtain an Euclidean signature, otherwise the third constraint in (F24) is nowhere satisfied for $\nu \in (0, 1)$.
- For $0 < \bar{e} \leq \frac{1}{2}$ (F24) is fulfilled $\forall \nu \in (0, 1)$. A simple analysis of (F23), considering the third constraint of (F24), shows that n is non-negative and attains every value in \mathbb{N} when ν varies in $(0, 1)$. Thus if $0 < \bar{e} \leq 1/2$, then for all positive integers n there exists $\nu \in (0, 1)$ so that (F23) and (F24) are fulfilled.
- For $\frac{1}{2} < \bar{e} < \frac{8}{5}$ the right-hand side of the third inequality in (F24) has a simple zero at some value $\nu^* \in (0, 1)$, thus the constraints (F24) are not fulfilled on $(0, \nu^*)$. Furthermore (F20) is required. As the third inequality in (F24) is a quadratic in the variable ν^2 , it is easy to verify that this condition holds on $(\nu^*, 1)$. For the interval $(\nu^*, 1)$ it follows from a

simple analysis that the function which at fixed \bar{e} assigns to ν the right-hand side of (F.23) attains every value in \mathbb{N} above some threshold $n_{\min}(\bar{e})$ and that the constraints are fulfilled. The zeros of the first derivative of (F.23) lead to a fifth order polynomial. Thus the minimum value can only be determined numerically. The result is illustrated in Figure F.1. From the numerical analysis it follows that $n = 4$ is the lowest

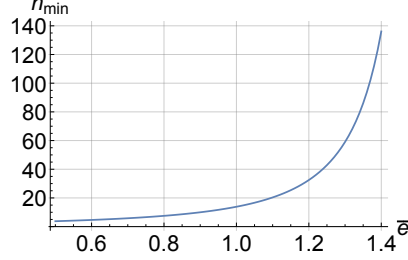


Figure F.1: The function $n_{\min}(\bar{e})$.

occurring “quantum number” for $\bar{e} \in (\frac{1}{2}, \frac{8}{5})$.

F.1.3 $\bar{e} < 0$

The addition of a negative charge increases the right-hand side of the third inequality in (F.24) $\forall \nu \in (0, 1)$. Thus from the analysis of the uncharged case, we can conclude that this constraint holds as well in the charged case. The right-hand side of the second inequality in (F.24) is monotonously decreasing in the uncharged case for $\nu \in (0, 1)$ and attains a zero at $\nu = 1$. The addition of a negative charge increases the rate of decreasing. From this it follows that there exists a zero of (F.15) located at $\nu^* \in (0, 1)$. Thus the constraints are fulfilled, for a given negative charge parameter, if and only if $\nu \in (0, \nu^*)$.

The numerator of the n -function (F.15) has no zeros on $(0, \nu^*)$, which follows from the second constraint in (F.7). Thus it suffices to determine if, for a given parameter \bar{e} , the maximum $n_{\max}(\bar{e})$ of the function of ν defined by the right-hand side of (F.23), for $\nu \in (0, \nu^*)$, is greater than or equal to one. This analysis can be carried out numerically. The result is illustrated in the plot F.2. From the numerical analysis we conclude, that $\bar{e} \gtrsim -0.5$ is a necessary criterion for the existence of a solution, and that $n = 1$ is the only possibility when $\bar{e} \leq 0$.

F.2 The Maxwell fields in the Page limit

In this section we analyse the regularity of the one-form (2.6) after passage to the limit $\epsilon \rightarrow 0$. The coordinate transformations (F.1)-(F.3) yield the following form for the p-contribution of (2.6) in $(\eta, \chi, \theta, \bar{\varphi})$ coordinates:

$$\begin{aligned} A^{(p)} &:= \frac{p \cos(\theta)}{\Sigma} \sigma_1 \\ &= \frac{p \cos(\theta)}{\Xi \Sigma} \left(a \omega_0 \left(\frac{-2r_0 \cos(\chi) + O(\epsilon)}{r_0^2 - a^2} \right) d\eta - (r^2 - a^2) d\bar{\varphi} \right). \end{aligned} \quad (\text{F.29})$$

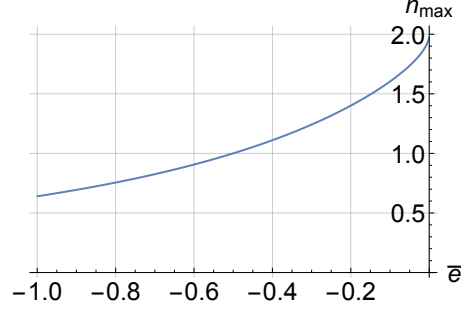


Figure F2: The function $n_{\max}(\bar{e})$.

Taking the Page limit, i.e. $\epsilon \rightarrow 0$, of (E29) gives

$$A^{(p)} = \frac{p \cos(\theta)}{\Xi \Sigma_{r_0}} \left(-\frac{2ar_0\omega_0 \cos(\chi)}{r_0^2 - a^2} d\eta - (r_0^2 - a^2) d\bar{\varphi} \right),$$

where

$$\Sigma_{r_0} = r_0^2 - a^2 \cos^2(\theta).$$

Near $\chi = 0$ we use the 2π -periodic coordinate ϕ , as introduced in analysis of the regularity of the metric, with corresponding coordinate differential (E8). This gives

$$\begin{aligned} A^{(p)} &= \frac{p \cos(\theta)}{\Xi \Sigma_{r_0}} \left(-\frac{2ar_0\omega_0 (\cos(\chi) - 1)}{r_0^2 - a^2} d\eta - \alpha(r_0^2 - a^2) d\phi \right) \\ &= \underbrace{\frac{p \cos(\theta)}{\Xi} \left(-\frac{2ar_0\omega_0 (\cos(\chi) - 1)}{\Sigma_{r_0} (r_0^2 - a^2)} d\eta + \frac{\alpha a^2 \sin^2(\theta)}{r_0^2 - a^2 \cos^2(\theta)} d\phi \right)}_{\text{smooth for } \chi < \pi} \\ &\quad - \frac{\alpha p \cos(\theta)}{\Xi} d\phi. \end{aligned} \quad (\text{F30})$$

As in Section 3.3, the last term is not smooth but the resulting Maxwell field is. We also note that the alternative potential

$$A^{(p)} + \frac{\alpha p}{\Xi} d\phi = A^{(p)} + \frac{p}{\Xi} \left(d\bar{\varphi} - \frac{2ar_0\omega_0}{(r_0^2 - a^2)^2} d\eta \right) \quad (\text{F31})$$

is smooth for $\chi < \pi$ and $\theta < \pi$, while

$$A^{(p)} - \frac{\alpha p}{\Xi} d\phi = A^{(p)} - \frac{p}{\Xi} \left(d\bar{\varphi} - \frac{2ar_0\omega_0}{(r_0^2 - a^2)^2} d\eta \right) \quad (\text{F32})$$

is smooth for $\chi < \pi$ and $\theta > 0$.

A similar analysis applies near $\chi = \pi$, and shows that the potential

$$A^{(p)} + \frac{\alpha p}{\Xi} d\hat{\phi} = A^{(p)} + \frac{p}{\Xi} \left(d\bar{\varphi} + \frac{2ar_0\omega_0}{(r_0^2 - a^2)^2} d\eta \right) \quad (\text{F33})$$

is smooth for $\chi > 0$ and $\theta < \pi$, while

$$A^{(p)} - \frac{\alpha p}{\Xi} d\hat{\phi} = A^{(p)} - \frac{p}{\Xi} \left(d\bar{\varphi} + \frac{2ar_0\omega_0}{(r_0^2 - a^2)^2} d\eta \right) \quad (\text{F34})$$

is smooth for $\chi > 0$ and $\theta > 0$.

The coordinate transformations (F1)-(F3) yield the following form for the e -contribution of (2.6) in $(\eta, \chi, \theta, \bar{\varphi})$ coordinates:

$$\begin{aligned} A^{(e)} &:= \frac{e r}{\Sigma} \sigma_2 \\ &= \frac{e r}{\Sigma \Xi} \left(-\frac{\omega_0}{\epsilon} \frac{r_0^2 - a^2 \cos^2(\theta)}{r_0^2 - a^2} d\eta + a \sin^2(\theta) d\bar{\varphi} \right) \\ &= \underbrace{\frac{e}{\Xi} \left(-\frac{\omega_0 r_0}{\epsilon(r_0^2 - a^2)} d\eta + \frac{\omega_0 \cos \chi}{(r_0^2 - a^2)} \left(1 - 2 \frac{r_0^2}{\Sigma} + O(\epsilon) \right) d\eta + \frac{a r}{\Sigma} \sin^2(\theta) d\bar{\varphi} \right)}_{\text{closed}}. \end{aligned}$$

The closed part has no limit as ϵ goes to zero but can be discarded without affecting the Maxwell field. Keeping the same symbol $A^{(e)}$ for the four-potential obtained after removing the singular term and taking the limit $\epsilon \rightarrow 0$, we find

$$A^{(e)} = \frac{e}{\Xi} \left[\frac{\omega_0 \cos(\chi)}{(r_0^2 - a^2)} \left(1 - \frac{2r_0^2}{\Sigma_{r_0}} \right) d\eta + \frac{a r_0}{\Sigma_{r_0}} \sin^2(\theta) d\bar{\varphi} \right].$$

Near $\chi = 0$ we use the 2π -periodic coordinate ϕ , as introduced in the analysis of the regularity of the metric, with corresponding coordinate differential (F8). This yields

$$A^{(e)} = \frac{e}{\Xi} \left[\frac{\omega_0 \cos(\chi)}{(r_0^2 - a^2)} \left(1 - \frac{2r_0^2}{\Sigma_{r_0}} \right) d\eta + \underbrace{\frac{a r_0}{\Sigma_{r_0}} \sin^2(\theta) \left(a d\phi - \frac{2a r_0 \omega_0}{(r_0^2 - a^2)^2} d\eta \right)}_{\text{smooth}} \right].$$

Similarly to (3.17) the *non-manifestly-smooth* part can be rewritten as:

$$\begin{aligned} &\frac{e \omega_0}{\Xi(r_0^2 - a^2)} \left[\left(1 - \frac{2r_0^2}{\Sigma_{r_0}} \right) \cos(\chi) - \frac{2a^2 r_0^2 \sin^2(\theta)}{\Sigma_{r_0}(r_0^2 - a^2)} \right] d\eta = \\ &\underbrace{\frac{e \omega_0}{\Xi(r_0^2 - a^2)} \left(1 - \frac{2r_0^2}{\Sigma_{r_0}} \right) (\cos(\chi) - 1) d\eta}_{\text{smooth for } \chi < \pi} - \underbrace{\frac{e \omega_0 (a^2 + r_0^2)}{\Xi(a^2 - r_0^2)^2} d\eta}_{\text{closed}}, \end{aligned} \quad (\text{F35})$$

which implies smoothness of the Maxwell field for $\chi < \pi$. We also see that the four-potential

$$A^{(e)} + \frac{e \omega_0 (a^2 + r_0^2)}{\Xi(a^2 - r_0^2)^2} d\eta \quad (\text{F36})$$

is smooth for $\chi < \pi$.

An analogous analysis near $\chi = \pi$, using the coordinate $\hat{\phi}$ of (F12), shows that the four-potential

$$A^{(e)} - \frac{e \omega_0 (a^2 + r_0^2)}{\Xi(a^2 - r_0^2)^2} d\eta \quad (\text{F37})$$

is smooth for $\chi > 0$.

F.3 Dirac strings

The results of Section F.2 can be summarised as follows: the potential

$$A + \frac{p}{\Xi} \left(d\bar{\varphi} - \frac{2ar_0\omega_0}{(r_0^2 - a^2)^2} d\eta \right) + \frac{e\omega_0(a^2 + r_0^2)}{\Xi(r_0^2 - a^2)^2} d\eta \quad (\text{F.38})$$

is smooth for $\chi < \pi$ and $\theta < \pi$; the potential

$$A - \frac{p}{\Xi} \left(d\bar{\varphi} - \frac{2ar_0\omega_0}{(r_0^2 - a^2)^2} d\eta \right) + \frac{e\omega_0(a^2 + r_0^2)}{\Xi(r_0^2 - a^2)^2} d\eta \quad (\text{F.39})$$

is smooth for $\chi < \pi$ and $\theta > 0$; the potential

$$A + \frac{p}{\Xi} \left(d\bar{\varphi} + \frac{2ar_0\omega_0}{(r_0^2 - a^2)^2} d\eta \right) - \frac{e\omega_0(a^2 + r_0^2)}{\Xi(r_0^2 - a^2)^2} d\eta \quad (\text{F.40})$$

is smooth for $\chi > 0$ and $\theta < \pi$; finally

$$A - \frac{p}{\Xi} \left(d\bar{\varphi} + \frac{2ar_0\omega_0}{(r_0^2 - a^2)^2} d\eta \right) - \frac{e\omega_0(a^2 + r_0^2)}{\Xi(r_0^2 - a^2)^2} d\eta \quad (\text{F.41})$$

is smooth for $\chi > 0$ and $\theta > 0$.

Recall that $\bar{\varphi}$ and η are 2π periodic, and that we have (see (F.14))

$$\frac{4|\omega_0|ar_0}{(r_0^2 - a^2)^2} = n \in \mathbb{N}^*. \quad (\text{F.42})$$

Repeating the usual arguments as in Section 7, the requirement of well defined charged Dirac fields implies existence of integers $\hat{n}_1, \hat{n}_2 \in \mathbb{Z}$ such that

$$\frac{2pq_0}{\hbar\Xi} = \hat{n}_1, \quad \frac{2\omega_0 e(a^2 + r_0^2)q_0}{\hbar\Xi(r_0^2 - a^2)^2} = \hat{n}_2, \quad (\text{F.43})$$

together with the constraint

$$\frac{4|\omega_0|par_0q_0}{\hbar\Xi(r_0^2 - a^2)^2} = \frac{n\hat{n}_1}{2} \in \mathbb{Z}. \quad (\text{F.44})$$

ACKNOWLEDGEMENTS: We are grateful to M.J. Duff for drawing our attention to [5]. Supported in part by the Austrian Science Fund (FWF) under project P 23719-N16 and by Narodowe Centrum Nauki under the grant DEC-2011/03/B/ST1/02625..

References

- [1] P.A.R. Ade et al., *Planck 2013 results. XVI. Cosmological parameters*, Astron. Astrophys. **571** (2014), A16.
- [2] B. Carter, *Hamilton-Jacobi and Schrödinger separable solutions of Einstein's equations*, Commun. Math. Phys. **10** (1968), 280–310. MR 0239841 (39 #1198)
- [3] P.T. Chruściel, J. Jezierski, and J. Kijowski, *Hamiltonian dynamics in the space of asymptotically Kerr-de Sitter spacetimes*, Phys. Rev. **D92** (2015), 084030, arXiv:1507.03868 [gr-qc].

- [4] P.T. Chruściel, C.R. Öz, and S.J. Szybka, *Space-time diagrammatics*, Phys. Rev. D **86** (2012), 124041, pp. 20, arXiv:1211.1718.
- [5] M.J. Duff and J. Madore, *Einstein-Yang-Mills pseudoparticles and electric charge quantization*, Phys. Rev. D (3) **18** (1978), 2788–2797. MR 511380 (80b:81072)
- [6] M. Dunajski, J. Gutowski, W. Sabra, and P. Tod, *Cosmological Einstein-Maxwell instantons and Euclidean supersymmetry: anti-self-dual solutions*, Classical Quantum Gravity **28** (2011), no. 2, 025007, 16, arXiv:1006.5149 [hep-th]. MR 2763408 (2011m:83083)
- [7] G.W. Gibbons and S.W. Hawking, *Cosmological event horizons, thermodynamics, and particle creation*, Phys. Rev. **D15** (1977), 2738–2751.
- [8] G.W. Gibbons and S.W. Hawking (eds.), *Euclidean quantum gravity*, World Scientific Publishing Co., Singapore, 1993.
- [9] A. Gomberoff and C. Teitelboim, *de Sitter black holes with either of the two horizons as a boundary*, Phys. Rev. **D67** (2003), 104024, arXiv:hep-th/0302204.
- [10] S.W. Hawking, *Gravitational instantons*, Phys. Lett. A **60** (1977), 81–83. MR 0465052 (57 #4965)
- [11] S.W. Hawking and S.F. Ross, *Duality between electric and magnetic black holes*, Phys. Rev. D (3) **52** (1995), 5865–5876, arXiv:hep-th/9504019. MR 1360435 (96i:83054)
- [12] E. Komatsu et al., *Seven-Year Wilkinson Microwave Anisotropy Probe (WMAP) Observations: Cosmological Interpretation*, Astrophys. Jour. Suppl. **192** (2011), 18 (47 pp.), arXiv:1001.4538 [astr-ph.CO].
- [13] H.K. Kunduri and J. Lucietti, *Classification of near-horizon geometries of extremal black holes*, Living Rev. Rel. **16** (2013), 8, arXiv:1306.2517 [hep-th].
- [14] F. Mellor and I. Moss, *Black Holes and Gravitational Instantons*, Class. Quantum Grav. **6** (1989), 1379–1385.
- [15] P. Orlik and F. Raymond, *Actions of the torus on 4-manifolds II*, Topology **13** (1974), 89–112.
- [16] D.N. Page, *A compact rotating gravitational instanton*, Phys. Lett. B **79** (1978), 235–238.
- [17] Planck collaboration, *Planck 2015 results. XIII. Cosmological parameters*, http://planck.caltech.edu/pub/2015results/Planck_2015_Results_XIII_Cosmological_Parameters.pdf.
- [18] J.F. Plebański and M. Demiański, *Rotating, charged, and uniformly accelerating mass in general relativity*, Ann. Phys. **98** (1976), 98–127. MR 0418838 (54 #6873)
- [19] Y. Sekiwa, *Thermodynamics of de Sitter black holes: thermal cosmological constant*, Phys. Rev. D (3) **73** (2006), 084009, 11, arXiv:hep-th/0602269. MR 2221379 (2006m:83087)